

This is to certify that the

dissertation entitled

Understanding Local Organization in Condensed Phases

presented by

John L. Delacruz

has been accepted towards fulfillment of the requirements for

Ph.D. degree in Chemistry

Date 9/17/02

MSU is an Affirmative Action/Equal Opportunity Institution

0-12771

LIBRARY Michigan State University

PLACE IN RETURN BOX to remove this checkout from your record.

TO AVOID FINES return on or before date due.

MAY BE RECALLED with earlier due date if requested.

DATE DUE	DATE DUE	DATE DUE

6/01 c:/CIRC/DateDue.p65-p.15

UNDERSTANDING LOCAL ORGANIZATION IN CONDENSED PHASES

Ву

John Leonard DelaCruz

A DISSERTATION

Submitted to
Michigan State University
in partial fulfillment of the requirements
for the degree of

DOCTOR OF PHILOSPHY

Department of Chemistry

2002

ABSTRACT

UNDERSTANDING LOCAL ORGANIZATION IN CONDENSED PHASES

By

John Leonard DelaCruz

We report on the reorientation dynamics of several Rhodamine chromophores in condensed phases. The purpose of these measurements is to gain a better understanding of local organization in condensed phases, which in turn will give a better understanding of a diverse range of phenomena such as local heating, solvation and energy transfer processes that occur on molecular length scales. We have employed a pump-probe picosecond laser spectrometer and a picosecond time-correlated single photon counting laser system in these studies to examine the chromophores in polar protic and aprotic condensed phases and anionic, cationic and neutral micellar systems. Specific environments include the n-alcohols, N,N-dimethylformamide, dimethyl sulfoxide, acetonitrile and the micellar systems of sodium dodecyl sulfate (SDS), cetyltrimethylammonium bromide (CTAB), and poly(ethylene) glycol dodecyl ether 400 (Thesit®). From the reorientation measurements on these molecules we have determined the effective rotor shape of the molecules in solution and the length scale upon which local heating occurs. We have also gained insight into the relationship between structure and local organization in condensed phases and the phenomenon of dielectric friction in polar environments. Lastly, we have gained an understanding of how organization in micellar environments occurs within the context of the ionic forces and the dispersive forces that comprise the micellar environment.

ACKNOWLEDGMENTS

I would like to thank my advisor, Professor Gary J. Blanchard for his unswerving dedication to my education and professional development, his wisdom when the problems became tough, his ability to step in at the right time and his dogged determination to stay away when warranted. Without his guidance, patience and humor, I might not have made it this far.

I would like to thank my mother, Bonnie Drapeau, my step-father, Louis J.

Drapeau, and my father, Leonard U.Y. DelaCruz for being supportive of my endeavors, no matter how crazy they sounded at the time and for believing in my ability even when I didn't.

Additionally, I would like to thank my group members in the Blanchard group, past and present for the humor, dedication, persistence and excellence that they have displayed. Good luck to everyone!

I'd like to specifically thank all of my close friends for the pleasure of their company, the stress relief and their ability to see the lighter side of life when things got tough.

Thank you to all of the professors, graduate students and staff members that I have had the pleasure of knowing at Michigan State University during the performance of my graduate work. Unfortunately you are too numerous to mention, but you will never be forgotten.

Thanks to all the members of the softball team for great moments off and on the field!

TABLE OF CONTENTS

LIST OF TABLES	vi
LIST OF FIGURES	vii
Chapter 1	1
Introduction	1
Literature Cited	11
Chapter 2	17
Introduction	
Experimental	
Chemicals and Sample Handling	20
Steady-sate spectroscopy	
Time-correlated single photon counting spectroscopy	
Results and Discussion	
Reorientation of the probe molecule	
Effective rotor shape	
Excitation-dependent reorientation dynamics	
Conclusions	
Literature Cited	
Chapter 3	44
Introduction	44
Experimental Section	47
Pump-Probe Laser System	47
Steady-Sate Spectroscopy	
Chemicals and Sample Handling	
Results and Discussion	
Linear optical response.	
Time resolved spectroscopy	
Debye-Stokes-Einstein equation.	
Reorientation of R610, R640 and R610 lactone.	
Reorientation of R700 and R800.	
Conclusions	
Literature Cited	
Chapter 4	72

Introduction	72
Experimental Section	75
Pump-probe laser system.	
Time-correlated single photon counting system.	
Steady-state spectroscopy.	
Chemicals and Sample Handling.	
Results and Discussion	
Linear optical response.	
Time resolved spectroscopy	
Wobbling-in-a-cone with translational diffusion and micelle rotation	93
Conclusion	
Literature cited.	97
Chapter 5	100
Conclusions and Future Work	100

.

LIST OF TABLES

Table 2.1 – Experimental Reorientation Times and Changes in Solution Viscosity and Temperature Associated with Internal Conversion of R640
Table 2.2 – Solvent Properties and Quantities Extracted from Transient Heating Calculations. The quantity $V_{thermal}$ is extracted from Δr and $V_{calc} = V_{solute} + V_{solvent}$, where these volumes are determined using Edward's method. Some values (*) of C_v are interpolated from literature data For the other alcohols
Table 3.1a. – Reorientation Times and Zero-Time Anisotropies for R610, R640 and R610 lactone in protic and aprotic solvents
Table 3.1b – Reorientation Times and Zero-Time Anisotropies for R700 and R800 in protic and aprotic solvents
Table 3.2. – Calculated dielectric friction times for Rhodamine 610 (R610) and 640 (R640). The times reported are intended to be additive contributions to the reorientation time calculated using the modified DSE model
Table 3.3. – Calculated molecular volumes and S0 permanent dipole moments for the rhodamines examined here. Volumes were calculated from Reference 57. Dipole moments were calculated using Hyperchem® v. 6.0 with PM-3 parameterization 60
Table 3.4. – Selected properties for the solvents used
Table 4.1 – Reorientation times and zero-time anisotropies for Rhodamine chromophores in aqueous and micellar environments
Table 4.2 – Various thermodynamic properties of Rhodamine chromophores in SDS and CTAB micellar environments
Table 4.3 – Wobbling constant (D _w) values for aqueous and D _w and θ ₀ micellar environments

LIST OF FIGURES

Figure 1.1 – Schematic of pump-probe laser spectrometer used in this work
Figure 1.2 – Schematic of the time-correlated single photon counting laser spectrometer used in this work.
Figure 2.1 – Structure of the Rhodamine 640 molecule, drawn as a free cation. Cartesian axes are indicated, with the π -plane defining the x-y plane
Figure 2.2 – Reorientation for R640 in the <i>n</i> -alcohols: (\blacksquare) indicates experimental data for excitation of the $S_1 \leftarrow S_0$ transition. The calculated DSE result for the stick limit ($f = 1$) is shown as the solid line and the calculated DSE result where $V = V_{\text{solute}} + 5V_{\text{solvent}}$ is indicated by the dashed line.
Figure 2.3 – Linear optical response of R640 in <i>n</i> -propanol. The spectra of R640 in other alcohols are similar. Wavelengths of excitation are 280 and 580 nm respectively. Absorption (solid line) and emission (dotted line) spectra are normalized for purposes of presentation.
Figure 2.4 – (a) Experimental instrument response and $I_{\parallel}(t)$ and $I_{\perp}(t)$ data for R640 excited at 580 nm ($S_1 \leftarrow S_0$) in <i>n</i> -propanol. (b) Experimental anisotropy function generated from data presented in (a). The best fit anisotropy decay function for this data set is $R(t) = (0.29 \pm 0.01) \exp(-t/(481 \pm 3 \text{ ps}))$ The residuals of the fit are shown in the inset.
Figure 2.5 – (a) Experimental instrument response and $I_{\parallel}(t)$ and $I_{\perp}(t)$ data for R640 excited at 290 nm ($S_2 \leftarrow S_0$) in n-propanol. (b) Experimental anisotropy function generated from data presented in (a). The best fit anisotropy decay function for this data set is $R(t) = (-0.09 \pm 0.01) \exp(-t/(383 \pm 12 \text{ ps}))$. The residuals of the fit are shown in the inset.
Figure 2.6 – Reorientation time dependence on solvent viscosity for excitation of the $S_1 \leftarrow S_0$ transition (\blacksquare) and the $S_2 \leftarrow S_0$ transition (\blacksquare).
Figure 3.1 – Structures of the five rhodamines studied here
Figure 3.2 – Absorption and emission spectra of (a) R610, (b) R640, in methanol 51
Figure 3.3 – Absorption and emission spectra of (a) R700, (b) R800, in <i>n</i> -propanol 52
Figure 3.4 – Absorption spectra of R610 lactone (solid line) in acetonitrile and ring- opened R610 lactone (dashed line) in methanol

Figure 3.5 – Calculated state energy levels for the rhoamines studied here. Calculations were performed at the semi-empirical level with PM-3 parameterization. State energies and oscillator strengths for $S_n \leftarrow S_0$ transistions were calculated using configuration interaction.
Figure 3.6 – Reorientation time constants of R610 (•) and R640 (o) as a function of solvent viscosity. The calculated DSE stick limit line is shown for each chromophore, with a dashed line for R610 and a dotted line for R610
Figure 3.7 – Reorientation time constants of ring-opened R610 lactone (•) and R610 (o) as a function of solvent viscosity. The calculated DSE stick limit lines are shown for each chromophore. For the ring-opened lactone, the calculated hydrodynamic volume reflects an increase due to ester formation
Figure 3.8 – Reorientation time constants of (a) R700 and (b) R800 as a function of solvent viscosity. Aprotic solvents are shown with open (\circ) circles and protic solvents are shown with open (\circ) squares. For each chromophore the calculated DSE stick and slip limit lines are shown.
Figure 4.1 – Rhodamines and surfactants used in this study. Top row, left to right: tetramethylrhodamine methyl ester (R1), tetramethylrhodamine ethyl ester (R2). Second row, left to right: tetraethylrhodamine hexyl ester (R6), tetraethylrhodamine octadecyl ester (R18). Third row: sodium dodecyl sulfate (SDS), Fourth row: cetyltrimethylammonium bromide (CTAB), Bottom row: polyethylene glycol 400 dodecyl ether (Thesit [®])
Figure 4.2 – Absorbance and fluorescence spectra of the rhodamine esters used in this study
Figure 4.3 – Time-resolved reorientation data for rhodamines in the aqueous phase. Squares (a) are experimental data points, and the solid line represents the theoretical reorientation calculated from the Debye-Stokes-Einstein equation
Figure 4.4 – Reorientation data for rhodamine aliphatic esters in aqueous SDS micelle solution. Biexponential anisotropy decay functions produced a) normalized prefactors for the contribution of the fast (o) and slow () components of the anisotropy decays. b) Reorientation time constants plotted as a function of increasing ester chain length 87
Figure 4.5 – Reorientation data for rhodamine aliphatic esters in aqueous CTAB micelle solution. Biexponential anisotropy decay functions produced a) normalized prefactors for the contribution of the fast (0) and slow (1) components of the anisotropy decays. b) Reorientation time constants plotted as a function of increasing ester chain length 88

Figure 4.6 – Reorientation data for rhodamine aliphatic esters in aqueous Thesit[®] micelle solution. Biexponential anisotropy decay functions produced a) normalized prefactors for the contribution of the fast (\circ) and slow (\blacksquare) components of the anisotropy decays. b) Reorientation time constants plotted as a function of increasing ester chain length. 89

Images in this dissertation are presented in color

Chapter 1.

Introduction

Understanding local organization in the solution phase has been a subject of considerable interest because of its effect on the process of solvation and the related phenomena of chemical reactions and intermolecular energy transfer. Despite almost three decades of nearly continuous investigation, the details of these solvent-solute interactions, particularly in polar solvent systems, remain to be understood in detail. 8-28

Condensed (liquid) phases are a widely used medium for chemical manipulation and reaction and a further understanding of intermolecular interactions that occur in these media would be of great value to the field of chemistry. Working in these phases presents unique challenges that must be met, such as rapidly changing spatial relationships between molecules and reaction time-scales that are often too rapid to be accessed by techniques such as x-ray diffraction and NMR spectroscopy. In condensed phases a combination of long-range forces, such as electronic and non-collisional energy transfer, occur over relatively long length scales, and short-time duration collisional phenomena, occurs and all of these processes contribute to the bulk behavior of the system. ²⁹⁻³³ Through the use of time-domain spectroscopies it has become possible to probe these interactions by measuring the molecular motion and energy relaxation processes that occur on these length and time scales.

With the development of picosecond lasers, the measurement of these phenomena has greatly expanded because many of the processes relevant to solvation occur on the picosecond or longer timescale, and this is especially true in polar, strongly associative

systems.^{8,22,23,34-36} From time-domain spectroscopic data, information can be extracted about how a molecule reorients in solution, and such results can then be analyzed within the framework of a well-developed model to gain insight into interactions of the molecule intuits its local environment.

Several different types of information are amenable to acquisition in the time-domain, including fluorescence lifetime,³⁷ molecular reorientation,³⁸⁻⁴¹ vibrational relaxation⁴ and transient fluorescence spectral shift measurements.^{8,9,24} Of these methods, molecular reorientation has proven to be among the most useful because of the generality of the phenomenon and the well-developed theoretical framework for the interpretation of the experimental data.

The starting point for interpreting molecular rotational motion measurements is usually the modified Debye-Stokes-Einstein (DSE) equation. 42,43

$$\tau_{OR} = \frac{\eta V f}{k_B T S} \tag{1.1}$$

This expression has proven remarkably useful in providing a semiquantitative model for rotational molecular motion in liquids. In this model, η is the solvent bulk viscosity, V is the solute hydrodynamic volume and the terms f and S are frictional boundary condition and solute molecular shape factors, respectively. This model assumes a continuum solvent and it has been shown to model reorientation data well in the limit that the individual solvent molecules are smaller than the solute.

A limitation to our understanding of motion in liquids is that we do not understand the solvent-solute boundary condition at the molecular level. A critical point in understanding the solvent-solute boundary condition is the notion of frictional interactions and "local" viscosity versus bulk viscosity.^{6,44,45} It is understood that the

viscosity experienced by the reorienting molecule may be quite different than that of the bulk liquid viscosity, but the exact transition point from local to bulk viscosity is often poorly understood or ill defined.

It has been recognized that the concept of mechanical friction as the sole contributor to mediating molecular reorientation, especially in polar and / or charged systems may be outdated and should be amended to include the concept of dielectric friction.^{29-33,46-53} In one model,³² dielectric friction can be best described by a dipole that is contained within a spherical cavity that is immersed into a dielectric fluid with a dielectric response that is frequency dependant. The dipole creates an electric field within the solvent, that is coupled to the dipole. If this dipole then rotates at some angular frequency, as in the case of rotational diffusion, an interaction will occur between the solvent dielectric and the electric field created by the dipole. However, because the solvent dielectric response is frequency dependant, a phase lag is generated between the dipole moment of the solute and the solvent dielectric. This phase lag induces a torque on the rotating dipole, thus leading to energy dissipation. This model was originally developed without any consideration of the hydrodynamic effects that occur in solution, but was later extended to incorporate these effects by Felderhof and others.⁵⁴ Alavi⁵⁵ extended this model by considering the dipole to be suspended among a distribution of point charges in a cavity. This model predicts values of dielectric friction that are much larger than those predicted by the point source model, and is a better model in that it allows closer agreement between theory and experiment. However, both models suffer from the same problem, which is that the conditions under which mechanical friction becomes less significant than dielectric friction are poorly understood.

Another area that has remained ill-defined is the effect of solute structure on intermolecular interactions and local organization. Exchanging one functional group for another to improve reactivity or solubility is a well established practice in organic chemistry, but our understanding of how and why these changes work often remains at an intuitive level. ^{20,25-28,56-63}

Micelles comprise another class of interesting, restricted motion environments where local organization is present. Information has been collected on the size, shape and formation of micelles. ⁶⁴⁻⁶⁷ It has been theorized that the forces that govern the formation of micelles are ionic and / or dipolar forces that are dominant in the head group region of the micelle and the hydrophobic dispersion forces that are dominant in the core region of the micelle. ⁶⁷⁻⁷² Clearly, these forces must exist in a balance or the formation of the micelle could not occur, but how the ionic forces and the van der Waal's forces interact remains an active area of interest. ^{71,73-84}

The Rhodamine family chromophores used in this dissertation provide excellent candidates to study local organization due to their ready solubility in a variety of polar and amphiphilic media and their high photo-stability and fluorescence quantum yield. They also provide a large variety of pendant functional groups from which the study of structure and functionality on local organization was facilitated.

The use of laser spectrometers has become common in the pursuit of these measurements and we present two such systems that have utilized in our work. The picosecond pump-probe laser spectrometer used for most of the laser based measurements has been described in detail elsewhere, ⁸⁶ and we present only a brief outline of its characteristics here. Figure 1.1 shows a mode-locked CW Nd:YAG laser

(Coherent Antares 76-S) that produces 30 W of average power (1064 nm, 100 ps pulses, 76 MHz repetition rate). The output of this laser is frequency doubled to produce ~3 W of average power at 532 nm, which is used to excite two cavity-dumped dye lasers (Coherent 702-3). The output of each dye laser is ~40-110 mW average power at an 8 MHz repetition rate with a pulse that produces a 7 ps FWHM autocorrelation trace using a three plate birefringent filter. The pump and probe wavelengths were chosen to access the $S_1 \leftarrow S_0$ transition of each chromophore to detect ground state population recovery. The probe laser polarization was set alternately to 0° and 90° relative to the pump laser polarization depending upon the experiment being performed. The detection of the transient signals was accomplished using a radio and audio frequency triple-modulation scheme, with synchronous demodulation detection. 87,88 Each reported time constant is the average of at least five individual determinations that are themselves the average of at least ten to twelve time-scans. A computer controlled interface controls a translation stage which, in turn, determines the arrival time of the probe pulse relative to that of the pump pulse, with the arrival time being determined by the distance that the translation stage travels. The time resolution of this system, ~10 ps is determined by the crosscorrelation between the pump and the probe laser pulse trains. Further information may be found in chapters 2 and 3 which detail our experiments using this laser system.

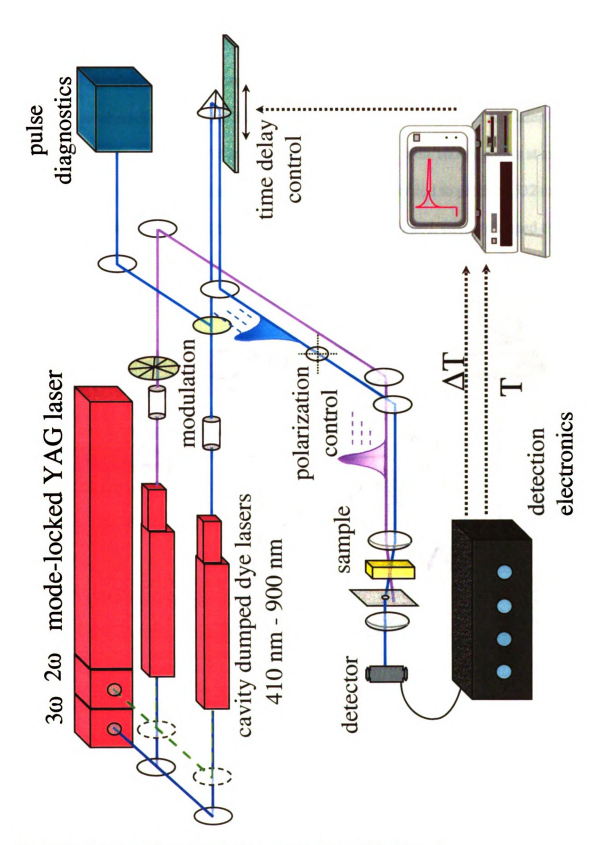


Figure 1.1 - Schematic of pump-probe laser spectrometer used in this work.

The time-correlated single-photon counting spectrometer used for the micellar and state dependent studies has been described elsewhere, ⁸⁹ and we present only a brief outline of its characteristics here. Figure 1.2 shows a mode-locked Nd:YAG laser (Quantronix 416) producing 7W average power at 1064 nm with 100 ps pulses at an 80 MHz repetition rate. The fundamental light is frequency doubled to produce 532 nm light which is used as an input to excite a synchronously pumped, cavity dumped dye

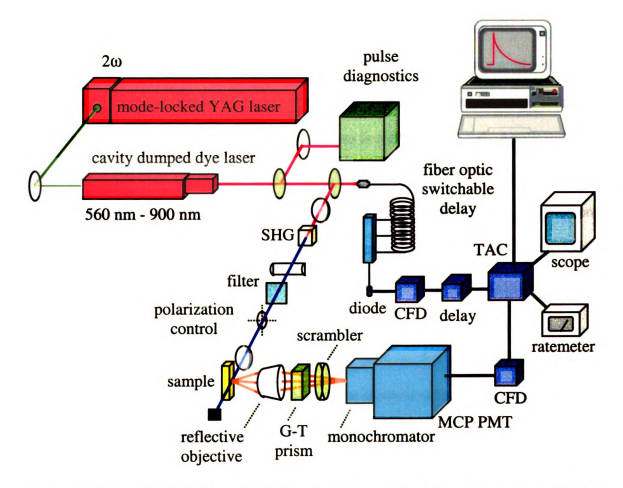


Figure 1.2 – Schematic of the time-correlated single photon counting laser spectrometer used in this work.

laser (Coherent 701-2) operating with Pyromethine 567 (Exciton) laser dye. The output of this laser is typically 80 mW average power with a 4 MHz repetition rate and 5 ps pulses.

Detection of the transient signals in this system was accomplished using a microchannel plate photomultiplier tube (Hamamatsu R3809U), where the light is collected by a microscope objective and filtered through a subtractive double monochromator (American Holographics DB-10). Further information may be found in chapters 2 and 4 of this dissertation which detail our experiments using this laser.

The study of dynamic interactions using rotational diffusion measurements is a widely used method to probe the nature of solvent-solute interactions, and the theoretical framework needed to understand these interactions is well documented. Application of the theory to the experimental data can provide information such as solute rotational diffusion constant, the dihedral angle between the excited and probed transition moments and in some cases, the dielectric properties of the local environment. The average local organization around the solute can then be inferred from the data and a picture can be formed of the solute-solvent interaction.

Using linearly polarized light, an ensemble of molecules with transition dipole moments oriented parallel to the polarization of the incident radiation can be excited and induce a transient anisotropy in the system. The induced anisotropy will decay in time due to the rotational dynamics of the system. The orientational anisotropy function can be extracted from the raw data through equation 1.2.

$$R(t) = \frac{I_{\parallel}(t) - I_{\perp}(t)}{I_{\parallel}(t) + 2I_{\perp}(t)}$$
 (1.2)

 $I_{\parallel}(t)$ and $I_{\perp}(t)$ are the intensities of the response when the polarizations are oriented either parallel or perpendicular to one another.

We have undertaken a series of studies in an attempt to better understand the effects of local organization on the process of solvation by examining the phenomena of local heating on short time scales, the effects of solute and solvent structure on local organization and the balance of forces that are present in organized structures such as micellar systems. We have used molecular reorientation, fluorescence lifetime and steady-state fluorescence measurements in condensed phases, and report our finding in this dissertation.

Chapter 2 of this dissertation outlines the steady state and time-resolved spectroscopy of Rhodamine 640 in a series of *n*-alcohols, methanol through decanol. From these studies we were able to form the framework from which the other studies proceeded in examining local organization around these chromophores. Qualitative assessments of the rotor shape, orientation of the ground and transition state dipole moments and a qualitative understanding of how the local environment changes were critical pieces of information for subsequent studies using this family of chromophores.

Chapter 3 of this dissertation details studies that were performed using a family of Rhodamines to better understand the effects of structural freedom on solvation and local organization. From these studies we have come to a better understanding of the effect of solvent on reorientation behavior. We were also able to come to better understand some of the forces that comprise these interactions.

Chapter 4 details a series of studies in micellar environments and an examination of the balance of forces that are present in these environments. From these studies we

were able to make qualitative and quantitative assessments of the micellar environment and how the organization present within these structures affects the reorientation behavior of the Rhodamine chromophores.

Chapter 5 provides some final conclusions as well as some suggestions for future work both with Rhodamines and in the condensed phase system that we have studied.

We draw some conclusion about the relationships between solute structure and local organization in the solvent systems that we have studied.

Literature Cited

- (1) Rasimas, J. P.; Blanchard, G. J. J. Phys. Chem. 1996, 100, 11526.
- (2) Rasimas, J. P.; Berglund, K. A.; Blanchard, G. J. J. Phys. Chem. 1996, 100, 7220.
- (3) Tulock, J. J.; Blanchard, G. J. J. Phys. Chem. A 2000, 104, 8340.
- (4) Goldie, S. N.; Blanchard, G. J. Phys. Chem. A 1999, 103, 999.
- (5) Rasimas, J. P.; Berglund, K. A.; Blanchard, G. J. J. Phys. Chem. 1996, 100, 17034.
- (6) Iwata, K.; Hamaguchi, H. J. Phys. Chem. A 1997, 101, 632.
- (7) DeWitt, L.; Blanchard, G. J.; LeGoff, E.; Benz, M. E.; Liao, J. H.; Kanatzidis, M. G. J. Am. Chem. Soc. 1993, 115, 12158.
- (8) Szabo, A. J. Chem. Phys. 1984, 81, 150.
- (9) von Jena, A.; Lessing, H. E. Chem. Phys. Lett. 1981, 78, 187.
- (10) Dutt, G. B.; Krishna, G. R. J. Chem. Phys. 2000, 112, 4676.
- (11) Dutt, G. B.; Srivatsavoy, V. J. P.; Sapre, A. V. J. Chem. Phys. 1999, 110, 9623.
- (12) Dutt, G. B.; Srivatsavoy, V. J. P.; Sapre, A. V. J. Chem. Phys. 1999, 111, 9705.
- (13) Dutt, G. B. J. Chem. Phys. 2000, 113, 11154.
- (14) Tao, T. Biopolymers 1969, 8, 609.
- (15) Chuang, T. J.; Eisenthal, K. B. J. Chem. Phys. 1972, 57, 5094.

- (16) Ferguson, J.; Mau, A. W. H. Chem. Phys. Lett. 1972, 17, 543.
- (17) Selwyn, J. E.; Steinfeld, J. I. J. Phys. Chem. 1972, 76, 762.
- (18) Kinosita Jr., K.; Kawato, S.; Ikegami, A. Biophys. J. 1977, 20, 289.
- (19) Porter, G.; Sadkowski, P. J.; Tredwell, C. J. Chem. Phys. Lett. 1977, 49, 416.
- (20) Sadkowski, P. J.; Fleming, G. R. Chem. Phys. Lett. 1978, 57, 526.
- (21) Spears, K. G.; Cramer, L. E. Chem. Phys. 1978, 30, 1.
- (22) von Jena, A.; Lessing, H. E. Chem. Phys. 1979, 40, 245.
- (23) von Jena, A.; Lessing, H. E. Ber. Bunsen-Ges. Phys. Chem. 1979, 83, 181.
- (24) Lipari, G.; Szabo, A. Biophys. J. 1980, 30, 489.
- (25) Hinckley, D. A.; Seybold, P. G.; Borris, D. P. Spectrochim. Acta, Part A 1986, 42, 747.
- (26) Hinckley, D. A.; Seybold, P. G. Spectrochim. Acta, Part A 1988, 44, 1053.
- (27) Barra, M.; Cosa, J. J.; de Rossi, R. H. J. Org. Chem. 1990, 55, 5850.
- (28) Sueishi, Y.; Sugiyama, Y.; Yamamoto, S.; Nishimura, N. Bull. Chem. Soc. Jpn. 1994, 67, 572.
- (29) Waldeck, D. H. The Role of Solute-Solvent Friction in Large-Amplitude Motions. In *Conformational Analysis of Molecules in Excited States*; Waluk, J., Ed.; Wiley-VCH, 2000; pp 113.
- (30) Simon, J. D. Acc. Chem. Res. 1988, 21, 128.
- (31) Su, S.; Simon, J. D. J. Phys. Chem. 1987, 91, 2693.

- (32) Nee, T.-W.; Zwanzig, R. J. Chem. Phys. 1970, 52, 6353.
- (33) Ladanyi, B. M.; Stratt, R. M. J. Chem. Phys. 1999, 111, 2008.
- (34) Bado, P.; Wilson, S. B.; Wilson, K. R. Rev. Sci. Instrum. 1982, 53, 706.
- (35) Andor, L.; Lorincz, A.; Siemion, J.; Smith, D. D.; Rice, S. A. Rev. Sci. Instrum. 1984, 55, 64.
- (36) Blanchard, G. J.; Wirth, M. J. Anal. Chem. 1986, 58, 532.
- (37) Kahlow, M. A.; Kang, T. J.; Barbara, P. F. J. Phys. Chem. 1987, 91, 6452.
- (38) Madden, P.; Kivelson, D. J. Phys. Chem. 1982, 86, 4244.
- (39) Moog, R. S.; Ediger, M. D.; Boxer, S. G.; Fayer, M. D. J. Phys. Chem. 1982, 86, 4694.
- (40) Philips, L. A.; Webb, S. P.; Clark, J. H. J. Chem. Phys. 1985, 83, 5810.
- (41) Philips, L. A.; Webb, S. P.; Yeh, S. W.; Clark, J. H. J. Phys. Chem. 1985, 89, 17.
- (42) Debye, P. Polar Molecules Chemical Catalog Co.: New York 1929.
- (43) Perrin, F. J. Phys. Radium 1934 5, 497.
- (44) Iwata, K.; Hamaguchi, H. J. Mol. Liq. 1995, 65/66, 417.
- (45) Iwata, K.; Hamaguchi, H. J. Raman Spectrosc. 1998, 29, 915.
- (46) Blanchard, G. J.; Cihal, C. A. J. Phys. Chem. 1988, 92, 5950.
- (47) Blanchard, G. J. J. Phys. Chem. 1988, 92, 6303.
- (48) Dote, J. L.; Kivelson, D. J. Phys. Chem. 1983, 87, 3889.

- (49) Jarzeba, W.; Walker, G. C.; Johnson, A. E.; Barbara, P. F. Chem. Phys. 1991, 152, 57.
- (50) Kivelson, D.; Spears, K. G. J. Phys. Chem. 1985, 89, 1999.
- (51) Kumar, P. V.; Maroncelli, M. J. Chem. Phys. 2000, 112, 5370.
- (52) Roy, K. I.; Lucy, C. A. Anal. Chem. 2001, 73, 3854.
- (53) Wiemers, K.; Kauffman, J. F. J. Phys. Chem. A 2000, 104, 451.
- (54) Felderhof, B. U. Mol. Phys. 1983, 48, 1283.
- (55) Alavi, D. S.; Waldeck, D. H. J. Chem. Phys. 1991, 94, 6196.
- (56) Rosenthal, I.; Peretz, P.; Muszkat, K. A. J. Phys. Chem. 1979, 83, 350.
- (57) Snare, M. J.; Treloar, F. E.; Ghiggino, K. P.; Thistlethwaite, P. J. J. Photochem. 1982, 18, 335.
- (58) Raue, R.; Harnisch, H.; Drexhage, K. H. Heterocycles 1984, 21, 167.
- (59) Preininger, C.; Mohr, G. J.; Klimant, I.; Wolfbeis, O. S. Anal. Chim. Acta 1996, 334, 113.
- (60) Watarai, H.; Funaki, F. Langmuir 1996, 12, 6717.
- (61) Pevenage, D.; Van der Auweraer, M.; De Schryver, F. C. Langmuir 1999, 15, 8465.
- (62) Kohn, F.; Hofkens, J.; De Schryver, F. C. Chem. Phys. Lett. 2000, 321, 372.
- (63) Ghanadzadeh, A.; Zanjanchi, M. A. Spectrochim. Acta, Part A 2001, 57, 1865.
- (64) Berr, S. S.; Caponetti, E.; Johnson, J. S.; Jones, R. R. M.; Magid, L. J. J. Phys. Chem. 1986, 90, 5766.

- (65) Berr, S. S.; Coleman, M. J.; Jones, R. R. M.; Johnson, J. S. J. J. Phys. Chem. 1986, 90, 6492.
- (66) Berr, S. S. J. Phys. Chem. 1987, 91, 4760.
- (67) Shitnitzky, M.; Dianoux, A.-C.; Gitler, C.; Weber, G. Biochemistry 1971, 10, 2106.
- (68) Jarzeba, W.; Walker, G. C.; Johnson, A. E.; Kahlow, M. A.; Barbara, P. F. J. Phys. Chem. 1988, 92, 7039.
- (69) Visser, A. J. W. G.; Vos, K.; van Hoek, A.; Santema, J. S. J. Phys. Chem. 1988, 92, 759.
- (70) Marcus, A. H.; Dichun, N. A.; Fayer, M. D. J. Phys. Chem. 1992, 96, 8930.
- (71) Quitevis, E. L.; Marcus, A. H.; Fayer, M. D. J. Phys. Chem. 1993, 97, 5762.
- (72) Cho, C. H.; Chung, M.; Lee, J.; Nguyen, T.; Singh, S.; Vedamuthu, M.; Yao, S.; Zhu, J.-B.; Robinson, G. W. J. Phys. Chem. 1995, 99, 7806.
- (73) Maiti, N. C.; Krishna, M. M. G.; Britto, P. J.; Periasamy, N. J. Phys. Chem. B 1997, 101, 11051.
- (74) Matzinger, S.; Hussey, D. H.; Fayer, M. D. J. Phys. Chem. B 1998, 102, 7216.
- (75) Riter, R. E.; Willard, D. M.; Levinger, N. E. J. Phys. Chem. B 1998, 102, 2705.
- (76) Willard, D. M.; Riter, R. E.; Levinger, N. E. J. Am. Chem. Soc. 1998, 120, 4151.
- (77) Pal, S. K.; Mandal, D.; Sukul, D.; Bhattacharyya, K. Chem. Phys. Lett. 1999, 312, 178.
- (78) Bhattacharyya, K.; Bagchi, B. J. Phys. Chem. A 2000, 104, 10603.
- (79) Pal, S. K.; Sukul, D.; Mandal, D.; Sen, S.; Bhattacharyya, K. Chem. Phys. Lett. **2000**, 327, 91.

- (80) Cang, H.; Brace, D. D.; Fayer, M. D. J. Phys. Chem. B 2001, 105, 10007.
- (81) Hara, K.; Kuwabara, H.; Kajimoto, O. J. Phys. Chem. A 2001, 105, 7174.
- (82) Sen, S.; Sukul, D.; Dutta, P.; Bhattacharyya, K. J. Phys. Chem. A 2001, 105, 7495.
- (83) Dutt, G. B. J. Phys. Chem. B 2002, 106, 7398.
- (84) Mandal, D.; Sen, S.; Bhattacharyya, K.; Tahara, T. Chem. Phys. Lett. 2002, 359, 77.
- (85) Drexhage, K. H. In *Dye Lasers*; 2nd ed.; Schaefer, F. P., Ed.; Springer: Berlin, 1977; pp 144.
- (86) Jiang, Y.; Hambir, S. A.; Blanchard, G. J. Opt. Commun. 1993, 99, 216.
- (87) Blanchard, G. J.; Wirth, M. J. Opt. Commun. 1985, 53, 394.
- (88) Blanchard, G. J.; Wirth, M. J. J. Chem. Phys. 1985, 82, 39.
- (89) Dewitt, L.; Blanchard, G. J.; Legoff, E.; Benz, M. E.; Liao, J. H.; Kanatzidis, M. G. J. Am. Chem. Soc. 1993, 115, 12158.

Chapter 2

Reorientation Dynamics of Rhodamine 640 in Normal Alcohols. Measurement of the Length and Time Scale of Transient Local Heating in Solution.

Introduction

Despite almost three decades of continuous investigation, the details of solvent-solute interactions, particularly in polar solvent systems, remain to be understood in detail. Most investigations of intermolecular interactions in solution have used a "probe" molecule present at low concentration in neat or binary solvent systems. Typically, a short pulse of light is used to establish some non-equilibrium condition in the ensemble of probe molecules, with the object of the experiment being to monitor the return of this population to equilibrium. Such studies have included fluorescence lifetime, molecular reorientation, 1-21 vibrational relaxation 22-34 and fluorescence spectral shift 35-44 measurements. Of these methods, molecular reorientation has proven to be among the most useful because of the combined generality of the effect and the well-developed theoretical framework for the interpretation of the experimental data. 45-50

The starting point for interpreting molecular rotational motion measurements is usually the modified Debye-Stokes-Einstein equation.^{46,47}

$$\tau_{OR} = \frac{\eta V f}{k_B T S} \tag{2.1}$$

In this model, τ_{OR} is the reorientation time constant (Chapter 1), η is the solvent bulk viscosity, V is the solute hydrodynamic volume, and the terms f and S are frictional boundary condition and solute molecular shape factors, respectively. This model assumes a continuum solvent and it has been shown to model reorientation data

quantitatively in the limit that the individual solvent molecules are smaller than the solute. One present limitation to our understanding of motion in liquids is that we do not understand the solvent-solute boundary condition at the molecular level. In the context of the modified DSE model, discrepancies between experiment and theory are often expressed in terms of the molecular-level breakdown of the notion of viscosity and in terms of the frictional coefficient, f, an empirical parameter.

The frictional term, f, is equal to unity in the so-called "stick" limit, which is taken as being representative of relatively strong solvent-solute interactions. For interactions weaker than the stick limit, the "slip limit" is used. ^{48,49} In this model, the strength of frictional interactions varies according to the shape of the molecule in such a way that 0 < f < 1. This model describes the behavior of non-polar molecules reorienting in nonpolar solvents well. In addition to frictional solvent-solute interactions, dielectric friction, arising from the dielectric response of the probe molecule and the environment can also contribute. ⁵¹⁻⁵³ For most systems, this contribution is small and in many cases difficult to define precisely owing to the limited information available on the local dielectric response of the probe molecule environment.

For polar solute molecules reorienting in polar solvents, it is common to recover experimental reorientation times that are substantially longer than those predicted by Eq. 2.1. This regime, referred to as "super-stick", remains ill defined but it is clear in such systems that strong intermolecular forces are responsible for the reorienting moiety not being simply the solute molecule, but rather the solute as well as some of the surrounding solvent cage. An additional uncertainty in such measurements lies in the determination of the solute shape factor, S. Perrin derived expressions for the term S to account for the

ellipsoidal shape of the solute rotor in solution.⁴⁶ These expressions depend on the shape of the solute and on the assumption of an effective rotor shape. The shape of the volume swept out by the probe molecule is, in many cases, unclear because of ambiguity about the details of the solute spectroscopic response and because of the limited information typically available from the experimental data.

Another issue that is rarely considered in molecular reorientation measurements is the local temperature of the solvent bath that is in closest proximity to the solute molecule. In the limit that the solute exhibits no Stokes shift and is characterized by an exclusively radiative decay, there is no reason to expect that the processes of excitation and de-excitation will deposit energy into the solvent bath. For organic fluorophores, where the fluorescence quantum yield is often on the order of 0.5 or less, and where Stokes shifts are at least hundreds of cm⁻¹, local heating must contribute to the experimental data at some level.

The work presented here addresses several limitations of the understanding of molecular motion in the liquid phase. The rotational diffusion behavior of the fluorescent probe molecule Rhodamine 640 (R640, Fig. 2.1 top) has been studied in a series of normal aliphatic alcohols, methanol through n-decanol. These experiments were performed using a time-correlated single photon counting apparatus that is capable of accessing both the $S_1 \leftarrow S_0$ and the $S_2 \leftarrow S_0$ transitions of R640. Data from these measurements reveal that R640 interacts strongly with multiple solvent molecules, giving rise to a reorienting moiety that is substantially larger than the hydrodynamic volume of the solute alone. By comparing the reorientation data taken for both excitation conditions, an unambiguous determination has been made that this probe molecule

reorients as a prolate rotor in normal alcohols, that the $S_1 \leftarrow S_0$ transition is polarized along the chromophore long axis (x) and the $S_2 \leftarrow S_0$ transition is polarized nominally orthogonal to the $S_1 \leftarrow S_0$ transition. Comparing the data taken for the two excitation conditions, we find direct evidence for local heating that results from the nonradiative dissipation of excitation energy from the S_2 to the S_1 state. The temperature rise was determined to be ~ 5 - 10 K and the manifestation of this effect depends on the solvent. The data shed new light on the timescale over which the thermal equilibration process occurs.

Experimental

Chemicals. Rhodamine 640 perchlorate was purchased from Exciton Chemical Company and used as received. All solvents were purchased from Aldrich Chemical Company in their highest grade available and used without further purification.

Steady state spectroscopy. Absorption spectra of the R640 solutions were measured with 1 nm resolution using a Cary 320 UV-visible absorption spectrometer. Fluorescence spectra were measured using a SPEX Fluorolog 3 spectrometer, also with 1 nm resolution.

Time correlated single photon counting spectroscopy. Fluorescence lifetime and rotational diffusion measurements were performed using a spectrometer that has been reported previously.⁵⁴ We provide a brief recap of its essential features here and a schematic of this system is shown in Figure 1.2. The source laser is a mode-locked Nd:YAG laser (Quantronix 416) producing 7 W average power at 1064 nm with 100 ps pulses at a 80 MHz repetition rate. The second harmonic of the output of this laser (532 nm, ~700 mW) is used to excite a synchronously pumped, cavity dumped dye laser

(Coherent 702-2) operating with Rhodamine 6G dye (Kodak). The output of this laser is typically 80 mW average power with a 4 MHz repetition rate and 5 ps pulses. For excitation of the $S_1 \leftarrow S_0$ transition, the 580 nm output of the dye laser was used to excite the sample directly. For excitation of the $S_2 \leftarrow S_0$ transition, the output of the dye laser was frequency-doubled using a Type I KDP crystal. Detection of the transient signals was accomplished using a microchannel plate photomultiplier tube (Hamamatsu R3809U), with fluorescence light collection through a reflecting microscope objective and wavelength selection with a subtractive double monochromator (American Holographics DB-10). The electronics used for signal processing are a Tennelec 455 quad constant fraction discriminator, 864 time-to-amplitude converter and biased amplifier. The reference channel was detected and delayed using an in-house built fiber optic delay line. The experimental signal was collected using a multichannel analyzer (PCA Multiport) and sent to a PC for processing. For this system, the instrument response function is typically 30-35 ps fwhm.

Results and Discussion

The central foci of this work are understanding the reorientation dynamics of R640 in the *n*-alcohols, methanol through *n*-decanol, and resolving the details of transient heating in solution associated with nonradiative relaxation subsequent to optical excitation. We consider three facets of the experimental data. The first is a comparison of our results to the predictions of the modified DSE model. The second issue we consider is the effective rotor shape swept out by the rotating probe molecule. This information is often not available unambiguously for probe molecules of low symmetry, such as R640, or for systems where the spectroscopy of the probe molecule is not

understood in detail. Finally, we consider the effect of initial excitation to different electronic states on the reorientation dynamics of this probe molecule.

Reorientation of the probe molecule. As discussed in the Introduction, the reorientation dynamics of probe molecules in solution are often treated using the modified DSE equation. This model is effective for cases where individual solvent molecules are small relative to the reorienting moiety, but in systems such as the ones we consider here, this approximation is clearly not valid. Alcohols are strongly associative liquids and the probe molecule, in its dissociated form, is a monocation. For these experimental conditions, it is not uncommon to find that the experimental reorientation dynamics are substantially slower than those predicted by the model.¹³ We find that to be the case for the data we present in Fig. 2.2. To our knowledge, there has not been a universally-accepted explanation for this experimental condition, although it is clear that slower than expected reorientation arises from strong solvent-solute interactions. In principle, according to Eq. 2.1, this phenomenon could be explained by an increase in viscosity, hydrodynamic volume or frictional coefficient, or an unexpected decrease in the value of S, the shape factor. From Perrin's equations, 46 the structure of R640 is found to have a shape factor of ~0.9 and the steric price that would have to be paid to make the shape factor ~0.2 would be prohibitive. A slower than expected reorientation time, if viewed in the context of a change in viscosity would suggest an increase in local viscosity, which is unlikely. The terms V and f are the variables most capable of accounting for the experimental data and, within the framework of the DSE model, values of f greater than unity are required to bring Eq. 2.1 into agreement with our data.

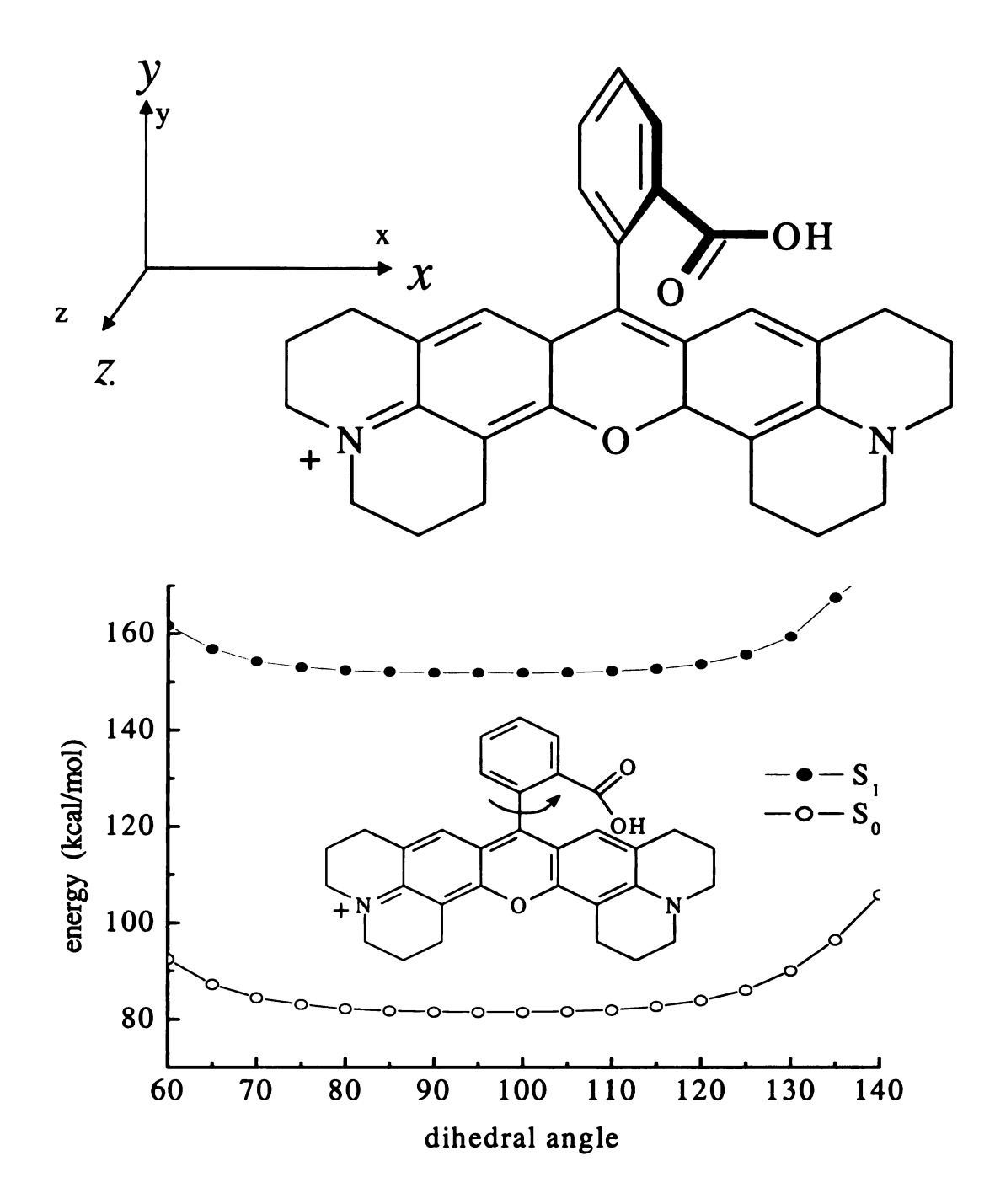


Figure 2.1 - Structure of the Rhodamine 640 molecule, drawn as a free cation. Cartesian axes are indicated, with the π -plane defining the x-y plane.

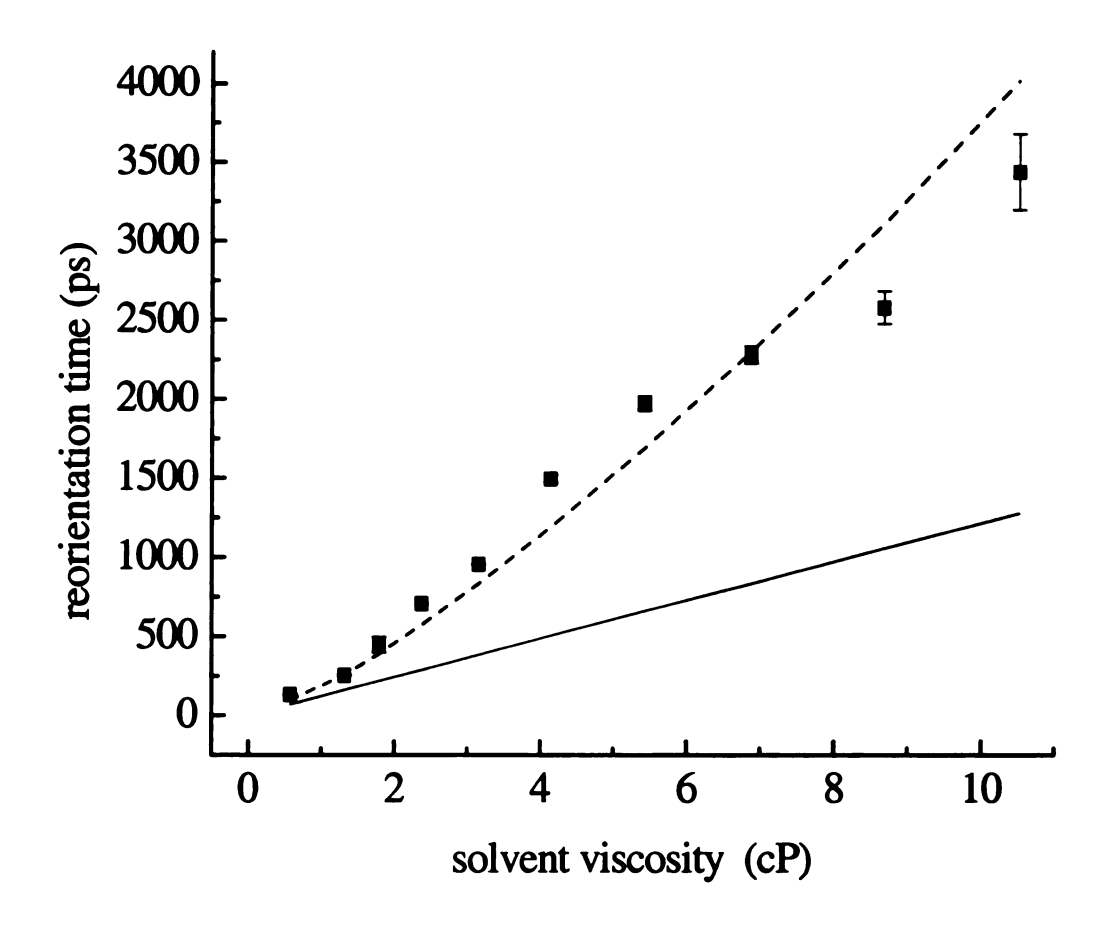


Figure 2.2 - Reorientation for R640 in the *n*-alcohols: (m) indicates experimental data for excitation of the $S_1 \leftarrow S_0$ transition. The calculated DSE result for the stick limit (f = 1) is shown as the solid line and the calculated DSE result where $V = V_{\text{solite}} + 5V_{\text{solite}}$ is indicated by the dashed line.

The most straightforward means to treat these data is based on the *ansatz* that the reorienting moiety observed experimentally is actually larger than that predicted by simple calculations of the hydrodynamic volume of the probe molecule. If this is the case, there are two possible ways to account for this finding. The first is to consider that the volume of the solute is larger (by a factor of two or more) than is calculated using Edward's model.⁵⁵ Intuition suggests that any increase of the solute volume is impractical, and the accuracy of molecular volumes calculated by Edward's method is well established. The second possible explanation for the data is that there is close

solvent association with the solute. 14,16 While it would not be appropriate to use the term "attachment" because of the implication of covalent bonds, strong association between the solute and some (average) number of solvent molecules, can produce reasonable agreement with the experimental data. The agreement between experiment and the model is best when the term $V = V_{\text{solute}} + 5V_{\text{solvent}}$. The viscosity-dependence of the reorientation time calculated using Eq. 2.1 with this value of V is in phenomenological agreement with the experimental data. Even better agreement between the model and experiment can be achieved if we choose only four solvent molecules for the longest alcohols but, given the level of detail contained in the experimental data, we are not justified in attempting such an empirical fit. Intuition suggests that there are four sites on the solute where polar solvent-solute interactions will be facile (Fig. 2.1), but the characteristic lifetime of such interactions is not known with certainty. Regardless of the exact number of solvent molecules closely associated with the solute, our reorientation data point to there being strongest interaction between the solute and a single layer of solvent molecules in the immediate proximity of the solute.

Effective rotor shape. The rotational motion of a molecule in solution is rarely consistent with the behavior expected of a spherical particle. For R640, the reorientation dynamics are not well characterized by modeling the effective rotor shape as a sphere. As noted above, we calculate a shape factor, S = 0.9, indicating a non-spherical probe shape. This value may be somewhat surprising given the way most rhodamine molecules are drawn. The reason for S being close to unity is that the phenyl ring substituent does not lie in the same plane as that of the fused ring structure. Semi-empirical calculations (Fig. 2.1, bottom) indicate a broad energetic minimum for this ring rotation angle

between ~70° and 125°, with substantial steric barriers (not shown) for structures approaching planarity.

To elucidate the intrinsically anisotropic nature of the molecular motion, Chuang and Eisenthal derived a series of equations that relate the spectroscopic and dynamical properties of the solute molecules to the form of the experimental data.⁴⁷

$$R(t) = \frac{I_{\parallel}(t) - I_{\perp}(t)}{I_{\parallel}(t) + 2I_{\perp}(t)} = \frac{6}{5} q_x q_y \gamma_x \gamma_y \exp(-(D_z + D)t) + \frac{6}{5} q_y q_z \gamma_y \gamma_z \exp(-(D_x + D)t) + \frac{6}{5} q_z q_x \gamma_z \gamma_x \exp(-(D_y + D)t) + \frac{3}{10} (\beta + \alpha) \exp(-(6D + 2\Delta)t) + \frac{3}{10} (\beta - \alpha) \exp(-(6D - 2\Delta)t)$$
(2.2)

 $I_{\parallel}(t)$ and $I_{\perp}(t)$ are the experimental signal intensities for fluorescence emitted at polarizations parallel and perpendicular, respectively, to the polarization of the excitation light. The terms q and γ are the Cartesian components of the unit vector describing the orientation of the excited and emitting transition dipole moments of the probe molecule, respectively. The terms D_x , D_y and D_z are the Cartesian components of the rotational diffusion constant and Δ is the average of these terms. The term β is related to the orientation of the transition moments and α is related to both the spectroscopic and motional properties of the system.

$$D = \frac{1}{3}(D_{x} + D_{y} + D_{z})$$

$$\Delta = \sqrt{(D_{x}^{2} + D_{y}^{2} + D_{z}^{2} - D_{x}D_{y} - D_{y}D_{z} - D_{z}D_{x})}$$

$$\beta = q_{x}^{2}\gamma_{x}^{2} + q_{y}^{2}\gamma_{y}^{2} + q_{z}^{2}\gamma_{z}^{2} - \frac{1}{3}$$

$$\alpha = (D_{x}/\Delta)(q_{y}^{2}\gamma_{y}^{2} + q_{z}^{2}\gamma_{z}^{2} - 2q_{x}^{2}\gamma_{x}^{2} + \gamma_{x}^{2} + q_{x}^{2}) +$$

$$(D_{y}/\Delta)(q_{z}^{2}\gamma_{z}^{2} + q_{x}^{2}\gamma_{x}^{2} - 2q_{y}^{2}\gamma_{y}^{2} + \gamma_{y}^{2} + q_{y}^{2}) +$$

$$(D_{z}/\Delta)(q_{x}^{2}\gamma_{x}^{2} + q_{y}^{2}\gamma_{y}^{2} - 2q_{z}^{2}\gamma_{z}^{2} + \gamma_{z}^{2} + q_{z}^{2}) - (2D/\Delta)$$

$$(2.3)$$

Using these equations, expressions for the induced orientational anisotropy, R(t), can be derived for either an oblate or a prolate ellipsoid under a variety of conditions relating to the orientations of the transition dipole moments. For the chromophore π system used to define the x-y plane.

Oblate: $D_z > D_x = D_y$

Prolate: $D_x > D_y = D_z$

There are several possible forms of the anisotropy decay and we summarize those relevant to this study below. For the $S_1 \leftarrow S_0$ transition, where the excited and emitting transition moments are nominally parallel to one another, and the transitions are polarized along the x axis, we obtain

$$R(t) = \frac{1}{10} \exp(-(2D_x + 4D_z)t) + \frac{3}{10} \exp(-6D_x t) \text{ (oblate)}$$
 (2.4)

and

$$R(t) = \frac{4}{10} \exp(-6D_z t) \qquad \text{(prolate)} \quad (2.5)$$

Conversely, if the transitions accessed are short-axis (y) polarized,

$$R(t) = \frac{1}{10} \exp(-(4D_x + 2D_z)t) + \frac{3}{10} \exp(-6D_x t)$$
 (prolate) (2.6)

and

$$R(t) = \frac{4}{10} \exp(-(4D_x + 2D_z)t)$$
 (oblate) (2.7)

For excitation of the $S_1 \leftarrow S_0$ transition in R640, we observe that the experimental R(t) function decays as a single exponential (Fig. 2.4). In principle, distinguishing between a one- and two-component decay can be difficult, however our experience from reorientation measurements on other systems has shown that determining the difference

between one and two decay components is straightforward, both in terms of the time constants and prefactors. 32,56

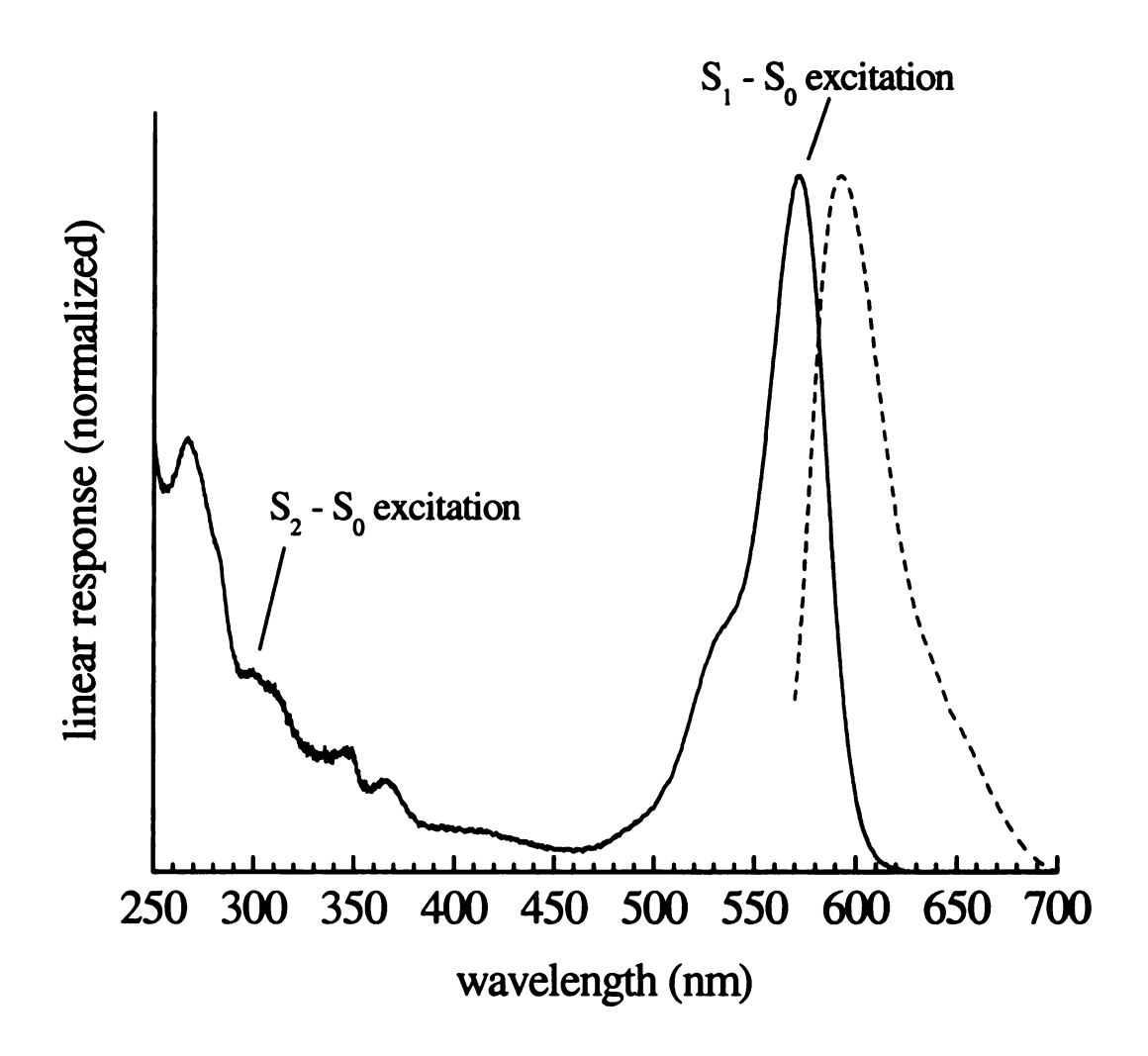


Figure 2.3 – Linear optical response of R640 in n-propanol. The spectra of R640 in other alcohols are similar. Wavelengths of excitation are 280 and 580 nm respectively. Absorption (solid line) and emission (dotted line) spectra are normalized for purposes of presentation.

Based on Eq. 2.4-2.7 we see, for a two-component decay, the prefactor for the minority constituent is 25% of the total. The residuals of the fits to the data demonstrate good agreement with a single exponential decay functionality (Fig. 2.4b inset). For systems of high symmetry, it is possible to assign the orientation of the transition moments but for systems such as the rhodamines, such an assignment is not possible with the requisite

certainty. Absent this knowledge, we are left with the ambiguous situation of not knowing if our molecule is characterized by a long-axis polarized transition and reorients as a prolate rotor or has a short-axis polarized transition and reorients as an oblate rotor.

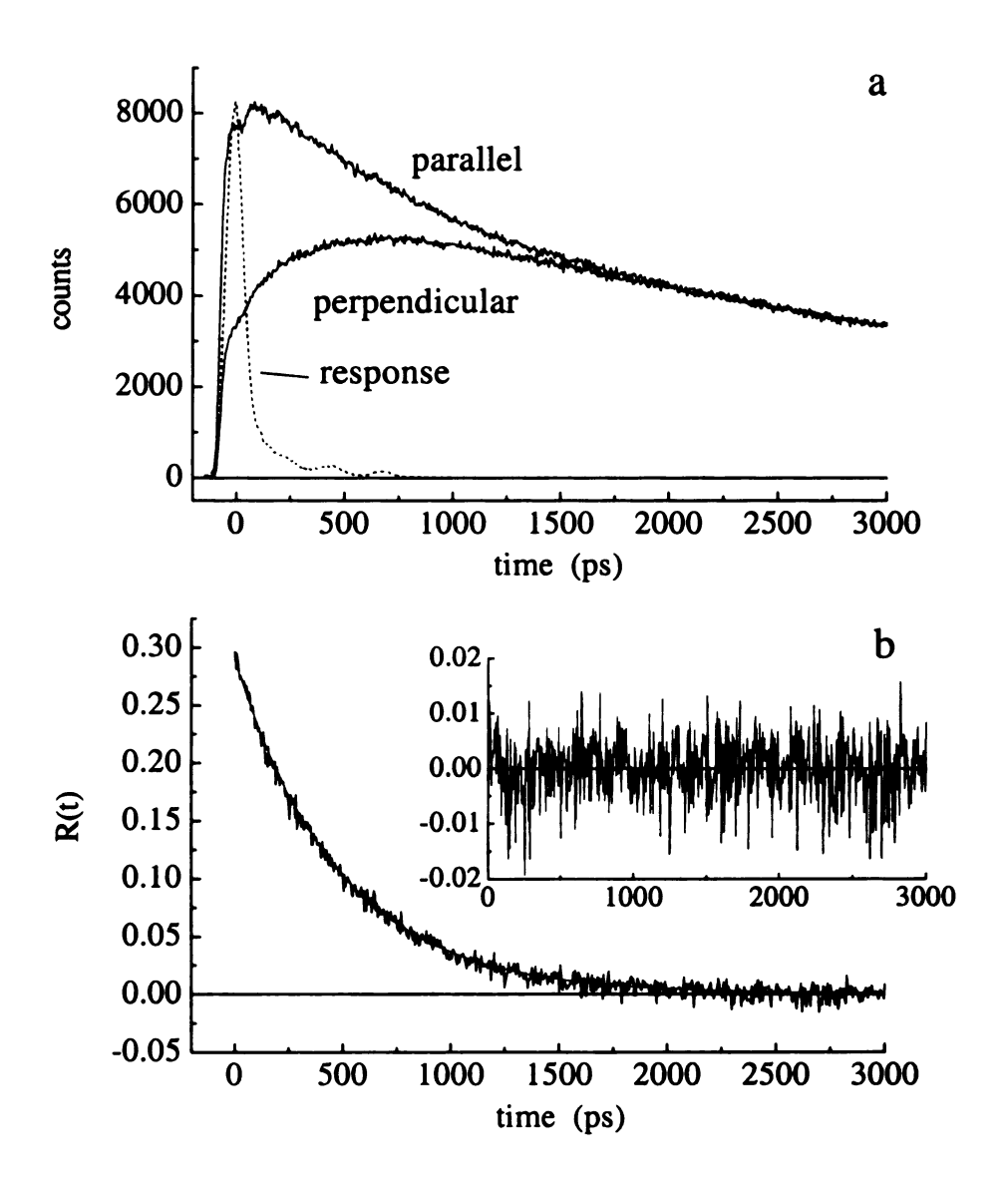


Figure 2.4 - (a) Experimental instrument response and $I_{\parallel}(t)$ and $I_{\perp}(t)$ data for R640 excited at 580 nm ($S_1 \leftarrow S_0$) in *n*-propanol. (b) Experimental anisotropy function generated from data presented in (a). The best fit anisotropy decay function for this data set is $R(t) = (0.29 \pm 0.01) \exp(-t/(481 \pm 3 \text{ ps}))$ The residuals of the fit are shown in the inset.

There has been discussion in the literature of the orientation of the transition moments for certain rhodamines,⁴ but this discussion was based on theoretical grounds and we are not aware of direct experimental verification.

We do have a means to resolve this issue and, at the same time, to provide unambiguous assignment of the transition polarizations in R640. For R640, as with many optical chromophores, the $S_2 \leftarrow S_0$ transition is polarized nominally perpendicular to the $S_1 \leftarrow S_0$ transition. We show the absorption and emission spectra of R640 in Fig. 2.3. For this condition, the expected form of R(t) for a prolate rotor is

$$R(t) = -\frac{2}{10} \exp\left[-6D_z t\right] \tag{2.8}$$

and for an oblate rotor,

$$R(t) = \frac{1}{10} \exp(-6D_x t) - \frac{3}{10} \exp(-(2D_x + 4D_z)t)$$
 (2.9)

By exciting the $S_2 \leftarrow S_0$ transition in R640 and monitoring emission from the S_1 state, we obtain an experimental R(t) function that decays as a single exponential (Fig. 2.5). As predicted from Eq. 2.8 and 2.9, we observe a negative zero-time anisotropy, a characteristic signature of transitions polarized nominally perpendicular to one another. The functionality of this anisotropy decay and that of the S_1 excitation experiment demonstrates unambiguously that R640 in the alcohols reorients as a prolate rotor. Because both excitation schemes sense the dynamics of R640 in the same state (S_1), then only Eq. 2.5 and 2.8 can be appropriate for our data. Specifically, our observation of a single exponential decay for S_1 excitation (Fig. 2.4) shows that either Eq. 2.5 or Eq. 2.7 is consistent with our data and that excitation of the $S_2 \leftarrow S_0$ transition (Fig. 2.5) produces a result that is consistent only with Eq. 2.8. These two pieces of information, taken

together, show that R640 reorients as a prolate rotor. Thus the $S_1 \leftarrow S_0$ transition in R640 must be long-axis (x) polarized and the $S_2 \leftarrow S_0$ transition is short axis (y) polarized.

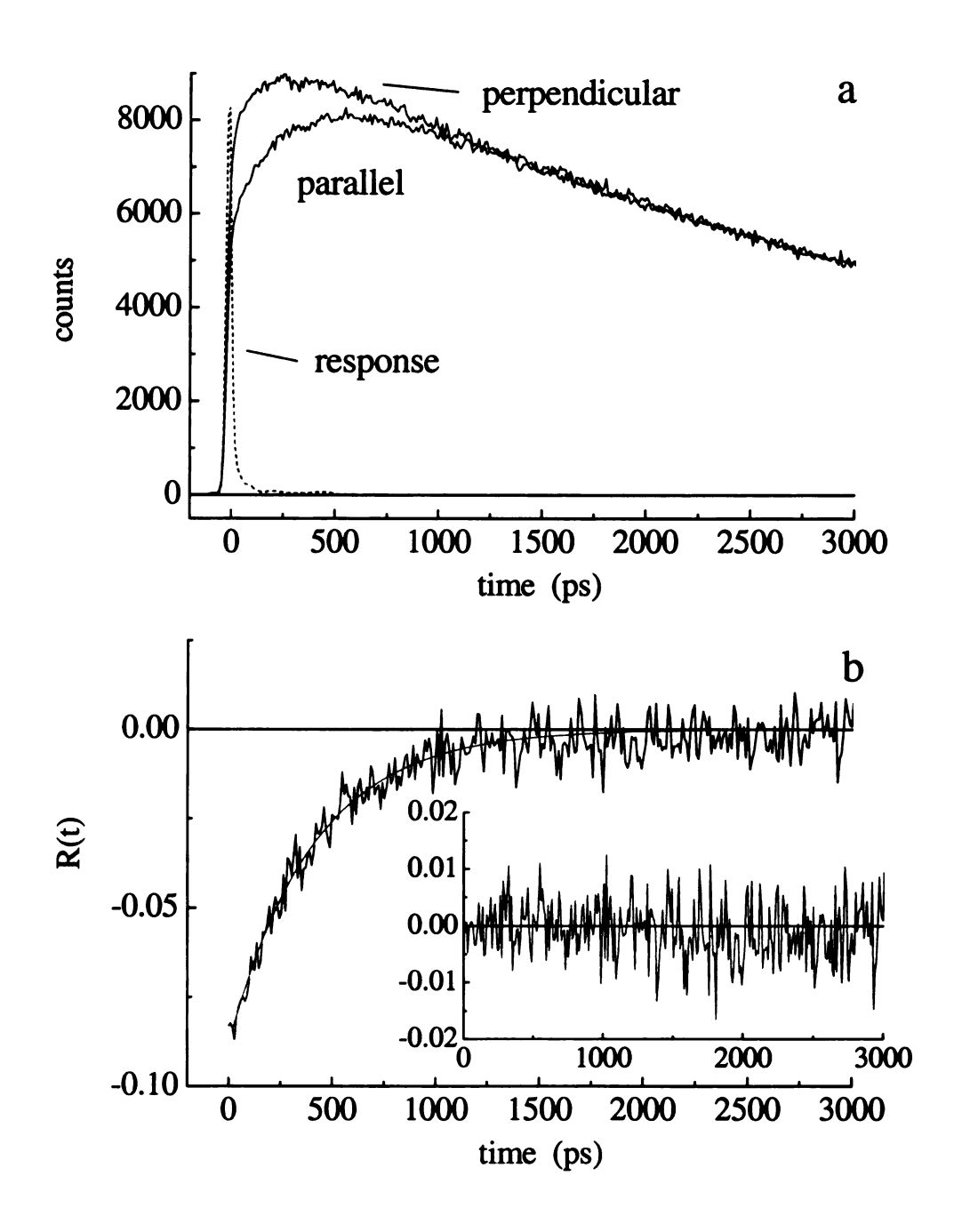


Figure 2.5 - (a) Experimental instrument response and $I_{\parallel}(t)$ and $I_{\perp}(t)$ data for R640 excited at 290 nm ($S_2 \leftarrow S_0$) in *n*-propanol. (b) Experimental anisotropy function generated from data presented in (a). The best fit anisotropy decay function for this data set is $R(t) = (-0.09 \pm 0.01) \exp(-t/(383 \pm 12 \text{ ps}))$. The residuals of the fit are shown in the inset.

Excitation-dependent reorientation dynamics. A closer examination of the reorientation data provides even greater insight into the energy dissipation dynamics operating in this system. A comparison of Eq. 2.5 and 2.8 reveals that the Cartesian component of the rotational diffusion constant sensed by both measurements is the same; the experimental time constant $\tau = \frac{1}{6D_{\tau}}$. This is not a surprising result, given the fact that we are observing motional relaxation from the S₁ state in both cases and it is well established that relaxation from the S₂ to the S₁ manifold is fast for complex organic molecules. We present the solvent-dependent reorientation times for excitation of both the S_1 and S_2 states in Fig. 2.6. These data demonstrate an interesting effect. For small solvents, such as methanol and ethanol, and for large solvents, such as n-nonanol and ndecanol, we observe the same experimental reorientation times for excitation of either S₁ or S_2 . For R640 in the intermediate solvents *n*-propanol through *n*-octanol, however, we measure reorientation times for S_2 excitation that are faster than those for S_1 excitation. This result is reproducible and appears to be inconsistent with the theory put forth in Eq. 2.2 - 2.9. Because we are measuring the dynamics of the same state of R640 for both sets of data, the volume and shape of the probe as well as the solvent-solute boundary condition must be the same for both sets of experiments. The only quantities that could change as a result of the different excitation conditions are the temperature and the viscosity of the environment in the immediate proximity of the probe molecule. We believe that both of these quantities change and discuss our basis for this assertion below.

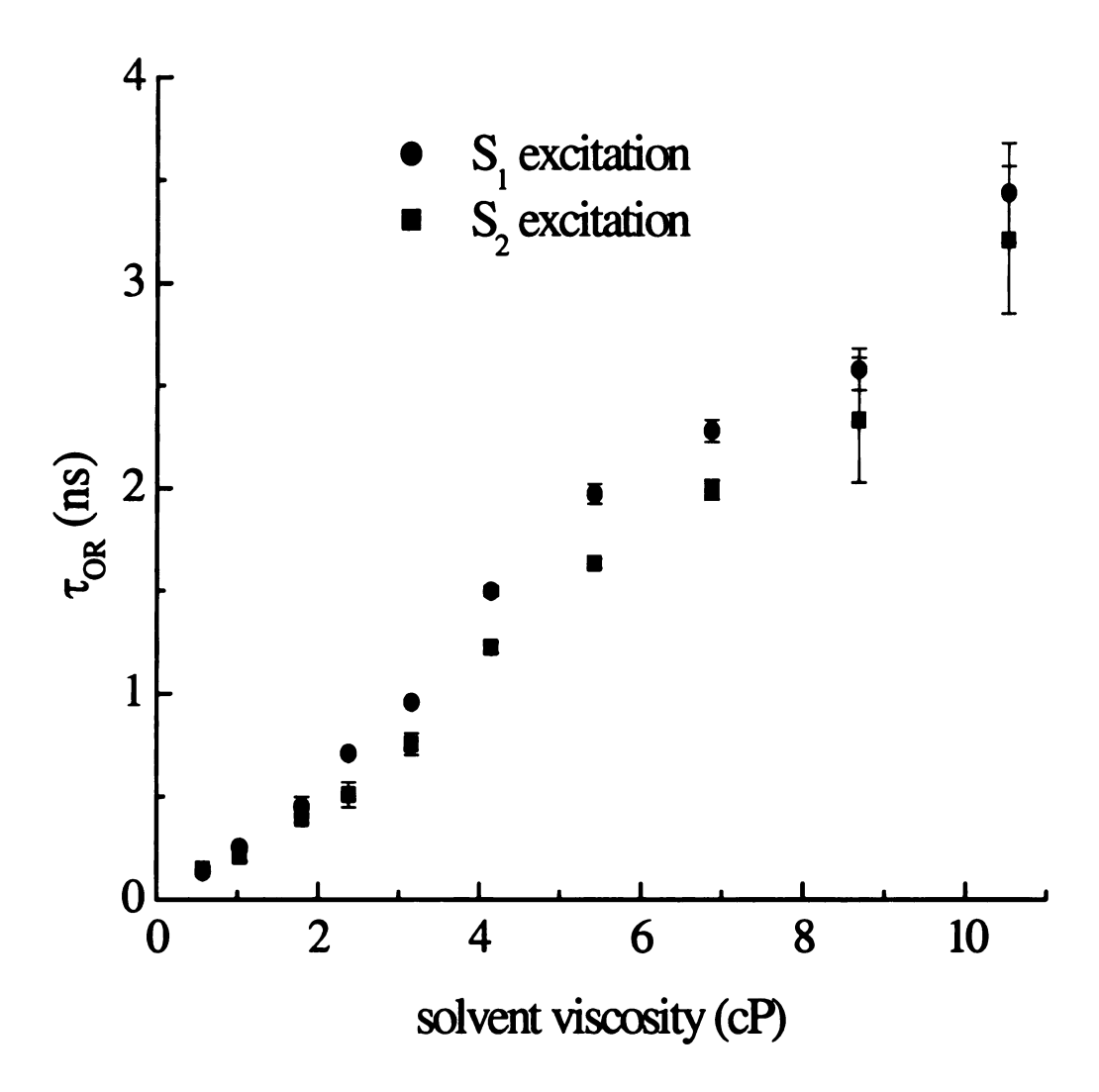


Figure 2.6 - Reorientation time dependence on solvent viscosity for excitation of the $S_1 \leftarrow S_0$ transition (\blacksquare) and the $S_2 \leftarrow S_0$ transition (\blacksquare).

The only difference between the two series of experiments lies in the excitation wavelengths used (580 nm vs. 290 nm). Emission from the sample is identical for the two excitation conditions and thus the difference between the two experiments is the energy dissipated nonradiatively into the solvent bath. For excitation of the $S_1 \leftarrow S_0$ transition, the Stokes shift is modest and the difference between excitation and

observation wavelengths is on the order of 30 nm. Excitation at 580 nm is close to the origin for this band (Fig. 2.3). For excitation of the $S_2 \leftarrow S_0$ transition, the R640 molecule dissipates ~ 2.1 eV of energy by nonradiative relaxation from S_2 to S_1 , an amount of energy sufficient to cause local heating. Such a phenomenon would give rise to a reduction in the viscosity and through this change, the reorientation time constant of the solute will decrease. Based on the magnitude of the decrease in reorientation time for excitation of the S_2 state, we can estimate the change in temperature using the following strategy. From Eq. 2.1, we can relate the state-dependence of the reorientation time to the transient change in viscosity. The bulk viscosity of liquids can be modeled phenomenologically and from this model we can relate the change in viscosity inferred from the reorientation data to the change in temperature sensed by the experimental measurement. Using the phenomenological change in temperature and knowing the amount of energy dissipated, we can estimate the effective distance over which temperature gradient persists. We describe each step in this process below.

Relating the change in reorientation time to the bulk solvent viscosity is accomplished through the modified DSE equation.

$$\Delta \tau_{OR} = \Delta \left(\frac{\eta}{T}\right) \left(\frac{Vf}{k_B S}\right) \approx \left(\frac{\Delta \eta Vf}{k_B T S}\right) \tag{2.10}$$

In this model, both the viscosity and the temperature are subject to change. We assert that the dominant contribution to $\Delta \tau_{OR}$ is $\Delta \eta$ and not ΔT . The reorientation time changes at most ~15% while the temperature change consistent with this result is on the order of a 3% increase. Because the bulk viscosity depends sensitively on the temperature, it is $\Delta \eta$ that is primarily responsible for $\Delta \tau_{OR}$.

The bulk viscosity of liquids is well understood and has been modeled accurately in a number of different ways. The origin of the phenomenon of viscosity is the interaction between molecules as they translate past one another in solution. Attractive interactions between molecules impede their flow, and the energy required for this action to occur is termed the viscous flow energy. Solution viscosity is typically treated in the context of an activated process and, as such, it has a predictable temperature dependence. The details of the temperature dependence are determined by the viscous flow energy and the prefactor in an Arrhenius expression. Because this temperature dependence is different for each liquid, the most common approach is to characterize this functionality using a parameterized fit. One such expression of the relationship between η and T is, ⁵⁷

$$T = \frac{A}{\eta} - \eta B + C \tag{2.11}$$

where A, B and C are parameters used to match the experimental viscosity temperature dependence to the model. From Eq. 2.11, an empirical expression for the temperature dependence of the viscosity can be derived.

$$\left. \frac{d\eta}{dT} \right|_{T_0} = \frac{-\eta^2}{A + \eta^2 B} \tag{2.12}$$

where T_0 is the ambient temperature of the bulk liquid, We use the published parameters A and B to determine the quantity $d\eta/dT$. With this information and the quantity $\Delta\eta$ (Eq. 2.10), we can estimate ΔT (Table 2.1). The quantity ΔT is the estimate of transient heating that gives rise to the state-dependent reorientation dynamics we observe experimentally.

Table 2.1 – Experimental Reorientation Times and Changes in Solution Viscosity and Temperature Associated with Internal Conversion of R640.

Solvent	$\tau_{OR}(S_1)$	$\tau_{OR}(S_2)$	$\Delta \tau_{OR} (S_2 - S_1)$	Δη (cP)	ΔT (K)
	(ps)	(ps)	(ps)		
Methanol	134 ± 3	146 ± 14	12 ± 10	0.07 ± 0.06	-8.59 ± 7.36
Ethanol	254 ± 5	209 ± 23	-45 ± 17	-0.23 ± 0.09	11.9 ± 4.66
1-propanol	449 ± 49	393 ± 21	-56 ± 38	-0.26 ± 0.17	6.30 ± 4.11
1-butanol	709 ± 9	507 ± 61	-202 ± 44	-0.84 ± 0.18	12.6 ± 2.69
1-pentanol	958 ± 2	755 ± 52	-203 ± 37	-0.77 ± 0.14	7.50 ± 1.36
1-hexanol	1499 ± 23	1223 ± 26	-276 ± 25	-0.96 ± 0.09	6.60 ± 0.62
1-heptanol	1973 ± 47	1635 ± 23	-338 ± 37	-1.09 ± 0.12	5.74 ± 0.63
1-octanol	2280 ± 54	1993 ± 47	-287 ± 51	-0.86 ± 0.15	3.77 ± 0.66
1-nonanol	2580 ± 102	2334 ± 304	-246 ± 227	-0.70 ± 0.65	2.71 ± 2.51
1-decanol	3439 ± 241	3212 ± 358	-227 ± 305	-0.59 ± 0.80	2.11 ± 2.86

At this point we consider the significance of the temperature jump we extract from the experimental data. The excess energy deposited into the system is simply the difference in energy between the excitation energies used to pump the $S_2 \leftarrow S_0$ transition (290 nm) and the $S_1 \leftarrow S_0$ transition (580 nm). We calculate this energy difference to be 2.13 eV. This heating pulse occurs during the time required for the population to relax from the S_2 to S_1 states and this time is determined by the intramolecular relaxation time or the duration of the excitation pulse, whichever is longer. Because of the characteristically fast kinetics of internal conversion, we believe the time duration of the excitation pulse (5 ps) is limiting in this case. The heat pulse associated with internal conversion of R640 is related to the temperature gradient in the system according to Eq. $2.13.^{58}$

$$\frac{q}{t} = \kappa A \frac{dT}{dr} \tag{2.13}$$

where κ is the thermal conductivity of the bath, $\kappa = \eta C_v$, A is the "area" of the radiator, which we take as the area of the chromophore π system, and dT/dr is the temperature gradient in solution that is induced by dissipation of the excess excitation energy. We

take the heat pulse, q/t as the energy dissipated over the duration of the excitation pulse, q/t as the energy dissipated over the duration of the excitation pulse, q/t = 2.13 eV/5 ps =68 nW. The area of the radiator is that of the chromophore π -system, and we approximate the dimensions as 12 Å x 14 Å = 168 Å². The thermal conductivities of the bulk solvents are determined by their viscosity and heat capacity, and both of these quantities vary in a regular manner with solvent aliphatic chain length (Table 2.2). From these data we calculate dT/dr and, using the phenomenological ΔT determined from the reorientation experiments, we can estimate Δr (Table 2.2). With the value of Δr , we calculate the volume for the corresponding sphere and compare these results to the values of the hydrodynamic volume of the reorienting moiety consistent with the experimental data (Fig. 2.2, Table 2.2). What is immediately apparent from a comparison of the thermal gradient and hydrodynamic volume data is that, for low and high viscosity solvents, there is not a correspondence, while in the intermediate region, the agreement is reasonable. Where there is a correspondence, we note the similarity of the two volumes. It thus appears that the temperature gradient exists largely over a distance consistent with a single layer of solvent molecules. Those molecules in closest proximity to the chromophore will be the primary recipients of the excess energy. Solvent molecules beyond the solvent cage in the immediate proximity of the probe molecule are coupled strongly to the solvent bath and are thus characterized by the bulk temperature of the system. The solvents that deviate from this model do so for reasons that we understand.

Table 2.2 – Solvent Properties and Quantities Extracted from Transient Heating Calculations. The quantity $V_{thermal}$ is extracted from Δr and $V_{calc} = V_{solvent}$, where these volumes are determined using Edward's method. Some values (*) of C_v are interpolated from literature data for the other alcohols.

Solvent	η (cP)	C _v (J/mol K)	κ (J/m s K)	Δr (Å)	V _{thermal} (Å ³)	V_{calc} (Å ³)
Methanol	0.576	73.2	1.32	-1.2 ± 1.0		624
Ethanol	1.032	104.0	2.28	2.8 ± 1.1	92	709
1-propanol	1.796	135.6	3.92	2.6 ± 1.7	74	794
1-butanol	2.377	168.8	5.20	6.9 ± 1.5	1376	879
1-pentanol	3.160	200.7	6.88	5.4 ± 1.0	660	964
1-hexanol	4.146	233.0	9.01	6.2 ± 0.6	998	1049
1-heptanol	5.427	255.4*	11.3	6.8 ± 0.8	1317	1134
1-octanol	6.878	276.2	13.9	5.5 ± 1.0	697	1219
1-nonanol	8.685	315.0*	18.0	5.3 ± 4.8	623	1304
1-decanol	10.524	344.8*	21.7	4.8 ± 6.5		1389

It is well established that the n-alcohols are characterized by long dielectric relaxation times, ranging from <100 ps for methanol to ~ 2 ns for n-decanol. This anomalous property of the alcohols is attributed to the extensive H-bonded network these solvents form and it is this relaxation time that is related to solvent molecule exchange in the solvent cage surrounding the solute. In order to detect the thermal relaxation event, it is necessary to use a detection time window less than or on the order of the dielectric relaxation time. For the solvents methanol, ethanol and 1-propanol, we observe little or no excitation energy dependence to the reorientation time. We assert that the reason for this behavior is that exchange of solvent molecules in the solvent cage is fast relative to the time constant for reorientation, the effective time window over which we sense the transient temperature change. Thus, the solvent molecules heated initially by nonradiative transfer are lost to the bath rapidly and the temperature of the *average* solvent cage sensed by the reorienting moiety is close to that of the bulk solvent.

We also observe no excitation energy-dependence to the reorientation times for the longest chain solvents, n-nonanol and n-decanol. We believe that this finding is due

to two factors. First, the thermal conductivity of the *n*-alcohols increases with solvent aliphatic chain length because of the increased degrees of freedom in these molecules. Thus the energy transfer to the bath mode is most efficient for these solvents. The second factor is that the temperature we sense is averaged over the solute reorientation time. The reorientation of R640 is slowest in these solvents, affording the greatest time for dissipation of energy within the window of observation.

We note that we are not the first group to conclude that the transfer of (vibrational) energy from solute to the immediate solvent environment is facile. Iwata and Hamaguchi have found evidence from transient S₁ Raman spectra of stilbene in selected solvents that the transfer of vibrational energy between the solute and the first solvent sphere proceeds over a timescale that depends on solvent, but that is similar to the reorientation time constant of stilbene in these systems. Subsequent solvent-solvent energy transfer appears to proceed more slowly. Our findings are in excellent qualitative agreement with that work.

Conclusions

We have studied the reorientation behavior of the polar probe molecule R640 in the series of alcohols methanol through n-decanol. By measuring the reorientation dynamics after exciting to two different excited electronic states, we have determined unambiguously that this molecule reorients as a prolate rotor in these solvents. We have also determined that the $S_1 \leftarrow S_0$ transition is long-axis (x) polarized and the $S_2 \leftarrow S_0$ transition is short-axis (y) polarized for R640. Modeling these data in the context of the modified DSE model indicates that the interactions between solvent and solute are stronger than predicted by this model. The "super-stick" behavior seen for R640 in the n-

alcohols is consistent with that seen for other charged dye molecules in polar solvents and we can model these data in the context of close solute association with four to five solvent molecules. We take this finding to indicate that the reorienting moiety we observe in solution is a solvent-solute complex where the lifetime of the solvent-solute interactions are on the same order as the reorientation time.

Comparing the results of the reorientation measurements for the two different excitation conditions reveals the effects of transient heating in such measurements. We have found that the transient change in temperature associated with non-radiative relaxation from the S₂ to S₁ electronic states in R640 is on the order of 10 K. We observe this transient temperature change with the relaxation time of the thermal gradient to be on the same order as the reorientation time of the probe molecule and whenever this condition is not obtained, the thermal gradient is not manifest in our experimental data. This thermal gradient generated by excitation to the S₂ state appears to be dissipated over approximately one solvent shell.

Literature Cited

- (1) Sanders, M. J.; Wirth, M. J. Chem. Phys. Lett. 1983, 101, 361.
- (2) Gudgin-Templeton, E. F.; Quivetas, E. L.; Kenney-Wallace, G. A. J. Phys. Chem. 1985, 89, 3238.
- (3) von Jena, A.; Lessing, H. E. Chem. Phys. 1979, 40, 245.
- (4) von Jena, A.; Lessing, H. E. Ber. Bunsen-Ges. Phys. Chem. 1979, 83, 181.
- (5) von Jena, A.; Lessing, H. E. Chem. Phys. Lett. 1981, 78, 187.
- (6) Eisenthal, K. B. Acc. Chem. Res. 1975, 8, 118.
- (7) Fleming, G. R.; Morris, J. M.; Robinson, G. W. Chem. Phys. 1976, 17, 91.
- (8) Shank, C. V.; Ippen, E. P. Appl. Phys. Lett. 1975, 26, 62.
- (9) Miller, D. P.; Shah, R.; Zewail, A. H. Chem. Phys. Lett. 1979, 66, 435.
- (10) Gudgin-Templeton, E. F.; Kenney-Wallace, G. A. J. Phys. Chem. 1986, 90, 2896.
- (11) Blanchard, G. J.; Wirth, M. J. J. Phys. Chem. 1986, 90, 2521.
- (12) Blanchard, G. J. J. Chem. Phys. 1987, 87, 6802.
- (13) Blanchard, G. J. J. Phys. Chem. 1988, 92, 6303.
- (14) Blanchard, G. J.; Cihal, C. A. J. Phys. Chem. 1988, 92, 5950.
- (15) Blanchard, G. J. J. Phys. Chem. 1989, 93, 4315.
- (16) Blanchard, G. J. Anal. Chem. 1989, 61, 2394.
- (17) Alavi, D. S.; Hartman, R. S.; Waldeck, D. H. J. Chem. Phys. 1991, 95, 6770.
- (18) Hartman, R. S.; Alavi, D. S.; Waldeck, D. H. J. Phys. Chem. 1991, 95, 7872.
- (19) Jiang, Y.; Blanchard, G. J. J. Phys. Chem. 1994, 98, 6436.
- (20) Brocklehurst, B.; Young, R. N. J. Chem. Phys. 1995, 99, 40.
- (21) Pauls, S. W.; Hedstrom, J. F.; Johnson, C. K. Chem. Phys. 1998, 237, 205.

- (22) Elsaesser, T.; Kaiser, W. Ann. Rev. Phys. Chem. 1991, 42, 83.
- (23) Lingle Jr., R.; Xu, X.; Yu, S. C.; Zhu, H.; Hopkins, J. B. J. Chem. Phys. 1990, 93, 5667.
- (24) Anfinrud, P. A.; Han, C.; Lian, T.; Hochstrasser, R. M. J. Phys. Chem. 1990, 94, 1180.
- (25) Heilweil, E. J.; Casassa, M. P.; Cavanagh, R. R.; Stephenson, J. C. J. Chem. Phys. 1986, 85, 5004.
- (26) Heilweil, E. J.; Casassa, M. P.; Cavanagh, R. R.; Stephenson, J. C. Ann. Rev. Phys. Chem. 1989, 40, 143.
- (27) Heilweil, E. J.; Cavanagh, R. R.; Stephenson, J. C. Chem. Phys. Lett. 1987, 134, 181.
- (28) Heilweil, E. J.; Cavanagh, R. R.; Stephenson, J. C. J. Chem. Phys. 1989, 89, 230.
- (29) Hambir, S. A.; Jiang, Y.; Blanchard, G. J. J. Chem. Phys. 1993, 98, 6075.
- (30) Jiang, Y.; Blanchard, G. J. J. Phys. Chem. 1994, 98, 9411.
- (31) Jiang, Y.; Blanchard, G. J. J. Phys. Chem. 1994, 98, 9417.
- (32) Jiang, Y.; Blanchard, G. J. J. Phys. Chem. 1995, 99, 7904.
- (33) McCarthy, P. K.; Blanchard, G. J. J. Phys. Chem. 1995, 99, 17748.
- (34) McCarthy, P. K.; Blanchard, G. J. J. Phys. Chem. 1996, 100, 5182.
- (35) Shapiro, S. L.; Winn, K. R. Chem. Phys. Lett. 1980, 71, 440.
- (36) Maroncelli, M.; Fleming, G. R. J. Chem. Phys. 1987, 86, 6221.
- (37) Huppert, D.; Ittah, V. Chem. Phys. Lett. 1990, 173, 496.
- (38) Huppert, D.; Ittah, V.; Kosower, E. Chem. Phys. Lett. 1989, 159, 267.
- (39) Chapman, C. F.; Fee, R. S.; Maroncelli, M. J. Phys. Chem. 1990, 94, 4929.
- (40) Jarzeba, W.; Walker, G. C.; Johnson, A. E.; Barbara, P. F. Chem. Phys. 1991, 152, 57.
- (41) Wagener, A.; Richert, R. Chem. Phys. Lett. 1991, 176, 329.

- (42) Fee, R. S.; Milsom, J. A.; Maroncelli, M. J. Phys. Chem. 1991, 95, 5170.
- (43) Yip, R. W.; Wen, Y. X.; Szabo, A. G. J. Phys. Chem. 1993, 97, 10458.
- (44) Fee, R. S.; Maroncelli, M. Chem. Phys. 1994, 183, 235.
- (45) Debye, P. Polar Molecules Chemical Catalog Co.: New York 1929.
- (46) Perrin, F. J. Phys. Radium 1934 5, 497.
- (47) Chuang, T. J.; Eisenthal, K. B. J. Chem. Phys. 1972, 57, 5094.
- (48) Hu, C.; Zwanzig, R. J. Chem. Phys. 1974, 60, 4354.
- (49) Youngren, G. K.; Acrivos, A. J. Chem. Phys. 1975, 63, 3846.
- (50) Zwanzig, R.; Harrison, A. K. J. Chem. Phys. 1985, 83, 5861.
- (51) Madden, P.; Kivelson, D. J. Phys. Chem. 1982, 86, 4244.
- (52) Kivelson, D.; Spears, K. G. J. Phys. Chem. 1985, 89, 1999.
- (53) Philips, L. A.; Webb, S. P.; Clark, J. H. J. Chem. Phys. 1985, 83, 5810.
- (54) Dewitt, L.; Blanchard, G. J.; Legoff, E.; Benz, M. E.; Liao, J. H.; Kanatzidis, M. G. J. Am. Chem. Soc. 1993, 115, 12158.
- (55) Edward, J. T. J. Chem. Ed. 1970, 47, 261.
- (56) Goldie, S. N.; Blanchard, G. J. J. Phys. Chem. A 1999, 103, 999.
- (57) Riddick, J. A. Organic Solvents; Wiley: New York, 1986.
- (58) Bromberg, J. P. *Physical Chemistry*, 2nd ed.; Prentice Hall: Englewood Cliffs, 1984.
- (59) Garg, S. K.; Smyth, C. P. J. Phys. Chem. 1969, 69, 1294.
- (60) Iwata, K.; Hamaguchi, H. J. Mol. Liq. 1995, 65/66, 417.
- (61) Iwata, K.; Hamaguchi, H. J. Phys. Chem. A 1997, 101, 632.
- (62) Iwata, K.; Hamaguchi, H. J. Raman Spectrosc. 1998, 29, 915.

Chapter 3.

The Influence of Chromophore Structure on Intermolecular Interactions. A Study of Selected Rhodamines in Polar Protic and Aprotic Solvents.

Introduction

The interactions between molecules determine both the microscopic and bulk properties of essentially all solution phase systems. Achieving a detailed understanding of these interactions has proven to be an elusive task because of their strength and their characteristically short persistence time. The timescale of solvation phenomena in polar liquids is considered to be on the order of the longitudinal relaxation time of the solvent, and can range from ~ 100 fs for polar aprotic solvents to hundreds of picoseconds for high viscosity solvents characterized by strong hydrogen bonding. The process of measuring such phenomena usually requires the use of a chromophore that can be accessed using short light pulses, and the properties of the chromophore can have a substantial influence on the information obtained from the experiment. Owing to the complexity of these systems, much information in the literature must be considered valid for only a specific chromophore or, at best, a limited number of structurally similar systems. 3-11

The Rhodamines are a family of molecules that have been used extensively as dyes for fabrics, biological stains, water markers, probes for studies of molecular-scale processes in condensed phases and at interfaces, probes for host-guest interactions, and as laser dyes. The utility of this family of dye molecules stems from their characteristically strong absorption at visible wavelengths, relatively high fluorescence quantum yields and several-nanosecond fluorescence lifetimes. There are a substantial

number of rhodamines, ¹² with most of the structural variations being made with the intent of controlling optical properties such as absorption energy or fluorescence lifetime. While the rhodamines are versatile probe molecules, their structural features serve to complicate the interpretation of experimental data in many cases. For example, several rhodamines possess a pendant *o*-substituted phenyl ring, and both the substituents and ring orientation relative to the chromophore plane can influence the motional and spectroscopic properties of the molecule. The extent of structural freedom remains largely undetermined for this ring, as does its role in mediating excited state relaxation and motional properties.

We are interested in understanding the relationship between rhodamine structure, steady state spectroscopy and solution phase dynamics. It is our ultimate intent to use this family of molecules in interfacial and other sterically restricted environments, such as lipid bilayers and micelles. A prerequisite for working in such environments is the development of an understanding of the role of chromophore structure on the experimental data we will acquire. For this reason we have undertaken a study of several rhodamines in selected polar protic and aprotic solvents.

This study describes the steady state spectroscopy and orientational relaxation dynamics of 5 substituted rhodamines (Figure 3.1). Our data, in conjunction with semi-empirical calculations, indicate that, for several of these rhodamines, dipolar solvent-solute interactions play at least as significant a role as hydrogen-bonding interactions in determining reorientation dynamics, despite the significantly different timescales that are characteristic for these interactions.

R610 R640

$$CF_3$$
 $R610$ R800 N

Figure 3.1 - Structures of the five rhodamines studied here.

Experimental Section

Pump-Probe Laser System. The picosecond pump-probe laser spectrometer used in these reorientation measurements has been described in detail previously, 23 and we present only a brief synopsis of its operation here. A mode-locked CW Nd:YAG laser (Coherent Antares 76-S) produces 30 W of average power (1064 nm, 100 ps pulses, 76 MHz repetition rate). The output of this laser is frequency-doubled to produce ~3 W of average power at 532 nm. The second harmonic light is used to excite two cavitydumped dye lasers (Coherent 702) synchronously, with the output of both lasers being ~70 mW average power at 8 MHz repetition rate, producing ~7 ps fwhm autocorrelation trace using a three plate birefringent filter. The pump dye laser was operated using Pyromethine 567 dye (Exciton) at 549 nm (for R610 and ring-opened R610 lactone experiments) and 564 nm (for R640 experiments). For experiments on R700 and R800, the pump laser was operated using LDS698 dye (Exciton) (645 nm for R700, 682 nm for R800). The probe laser was operated with Rhodamine 6G dye (Kodak) at 564 nm (for R610 and ring-opened R610 lactone experiments) and 580 nm (for R640 experiments). Kiton Red dye (Exciton) was used in the probe laser for R700 and R800 chromophores (615 nm for R700, 622 nm for R800). The pump wavelength and probe wavelengths were chosen to access the $S_1 \leftarrow S_0$ transition of each chromophore to detect ground state population recovery. The probe laser polarization was set to 0° and 90° relative to the pump laser polarization for individual scans of parallel and perpendicular polarization used in acquiring orientational relaxation data. The time resolution of this system, ~10 ps, is determined by the cross-correlation of the pump and probe laser pulses. Detection of the transient signals was accomplished using a radio- and audio-frequency triplemodulation scheme, with synchronous demodulation detection. The reorientation time constants we report here are the average of 6 individual determinations, each comprised of the average of 10 - 12 sets of $I_{\parallel}(t)$ and $I_{\perp}(t)$ scans.

Steady-Sate Spectroscopy. The steady-state absorption spectra of the chromophores used here were recorded with 1 nm resolution using a Cary 300 Bio UV-visible spectrophotometer. The spontaneous emission spectra for the same solutions were obtained with 1 nm resolution using a SPEX Fluorolog-3 spectrometer. These data were compared to semi-empirical computational results (Hyperchem® v. 6.0) and were used to determine the appropriate pump and probe wavelengths for each chromophore / solvent combination.

Chemicals and Sample Handling. The probe molecules Rhodamine 610 (R610), Rhodamine 640 (R640), Rhodamine 700 (R700), and Rhodamine 800 (R800) were obtained from Exciton Chemical Co. and used as received. Rhodamine 610 lactone (R610 lactone) was obtained from Aldrich Chemical Co. and was used as received. All solvents except water were obtained from Aldrich (99+% purity) and were used without further purification. Distilled, deionized water was available in-house. The concentration of all solutions used for laser measurements was $10~\mu \underline{M}$. Measurements of R700 solutions were hampered by bleaching of the solution. This effect was mitigated by replacement with fresh solution on at least a daily basis, or as warranted. All measurements were taken using a flowcell with a 1 mm pathlength. Solution temperatures were maintained at 298 \pm 0.5 K (Neslab EX100-DD).

Results and Discussion

We are interested in using Rhodamines as probes of their local environment in a number of systems, such as bulk liquids, micelles, polymer matrices and interfacial adlayers. To make use of these chromophores, we must first understand their optical properties and the relationship(s) between chromophore structure and intermolecular interactions. We consider first the structure-dependence of the linear optical response of rhodamines, with an eye toward understanding experimental trends in the data. With that understanding in place, we will consider the reorientation dynamics of several rhodamines in polar protic and aprotic solvents. Our data point to the importance of dipolar solvent-solute interactions, a result that is unusual in comparison to the behavior of a variety of other chromophores.

Linear optical response. The normalized absorption and emission spectra of the chromophores studied here are shown in Figures 3.2 – 3.4. The absorption and emission spectra of R610 and R640 (Figure 3.2) are blue-shifted significantly from the spectra of R700 and R800, (Figure 3.3) and the experimental trend is mirrored in the results of semi-empirical calculations performed with a PM-3 parameterization (Figure 3.5). $^{27-30}$ As has been indicated by Drexhage, 22 the o-benzoate ring at the 1 position of R610 and R640 is effectively decoupled from the 3-ring chromophore system. For R800, we understand the red-shift in the context of an effective increase in the extent of the π -system to include the $-C \equiv N$ group. R700 is red-shifted from R610 and R640 because the fluorine 3p atomic orbitals on the $-CF_3$ group at the 1 position can interact with the chromophore π -system. $^{31-33}$ The π -interaction with the F 3p atomic orbitals is not on the same order as that for the $-C \equiv N$ π orbitals of R800, and the spectral response of R700 is

not shifted as far to the red. The linear optical response of R610 lactone is qualitatively different from that of the other rhodamines by virtue of the presence of the lactone ring.

34-38 Closure of the lactone ring at the 1 position breaks the conjugation of the chromophore system, giving rise to an absorption spectrum that is blue shifted by ~200 nm relative to R610 (Figure 3.4). In protic solvents, such as the primary *n*-alcohols used in this study, hydrolytic ester formation proceeds efficiently with the resultant formation of the rhodamine chromophore, and a steady state optical response identical to R610 (Figure 3.3). This is an expected and well-documented result. 36,39-42 With this understanding of the steady state optical properties of the rhodamines, we turn to an examination of the dynamical behavior of these chromophores.

Time resolved spectroscopy. Conversion of the experimental data ($I_{\parallel}(t)$ and $I_{\perp}(t)$) to the induced orientation anisotropy function, R(t), is accomplished using Eq. 3.1.

$$R(t) = \frac{I_{\parallel}(t) - I_{\perp}(t)}{I_{\parallel}(t) + 2I_{\perp}(t)}$$
(3.1)

The functionality of the R(t) decay provides important information on the dynamics of the chromophores. In this work, we find that all of the chromophores exhibit single exponential anisotropy decays and the $S_1 \leftarrow S_0$ transitions accessed spectroscopically are oriented along the rhodamine chromophore long axis. These pieces of information, taken together, indicate that all of the rhodamine probe molecules we use reorient as prolate rotors in the solvents studied. Because of the observed single exponential decay functionality, we can interpret our data in the context of the modified DSE equation (Eq. 3.2).

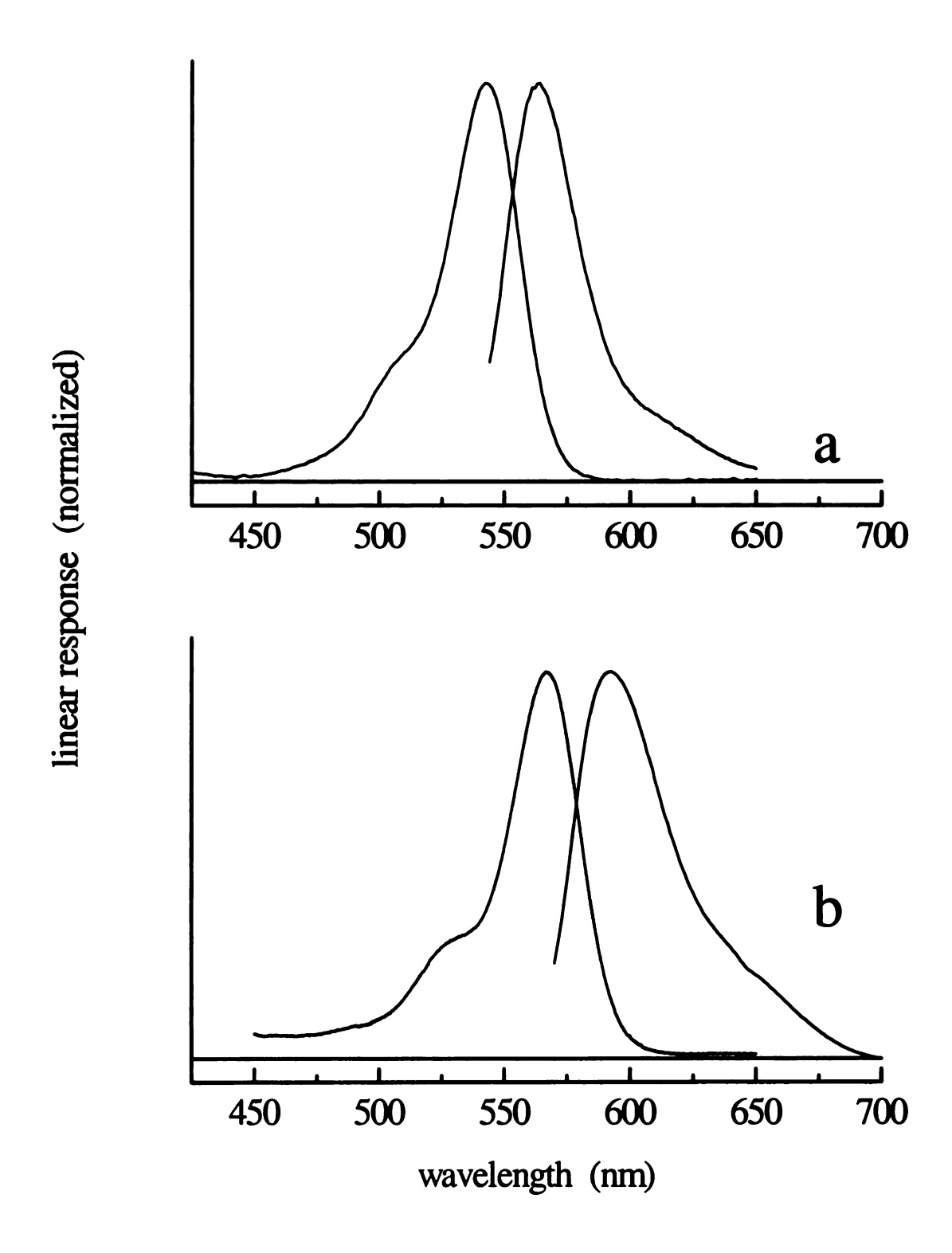


Figure 3.2 - Absorption and emission spectra of (a) R610, (b) R640, in methanol.

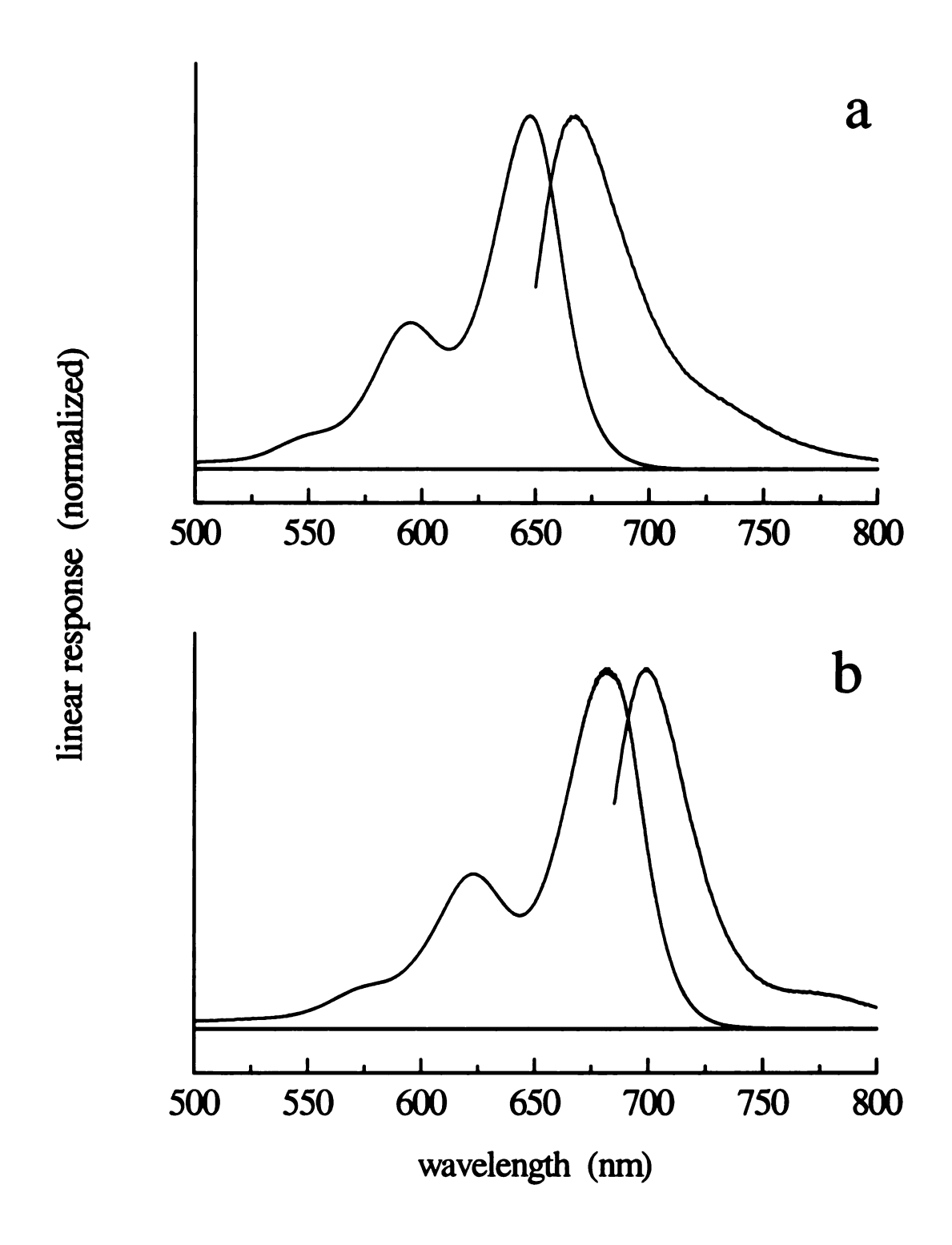


Figure 3.3 - Absorption and emission spectra of (a) R700, (b) R800, in *n*-propanol.

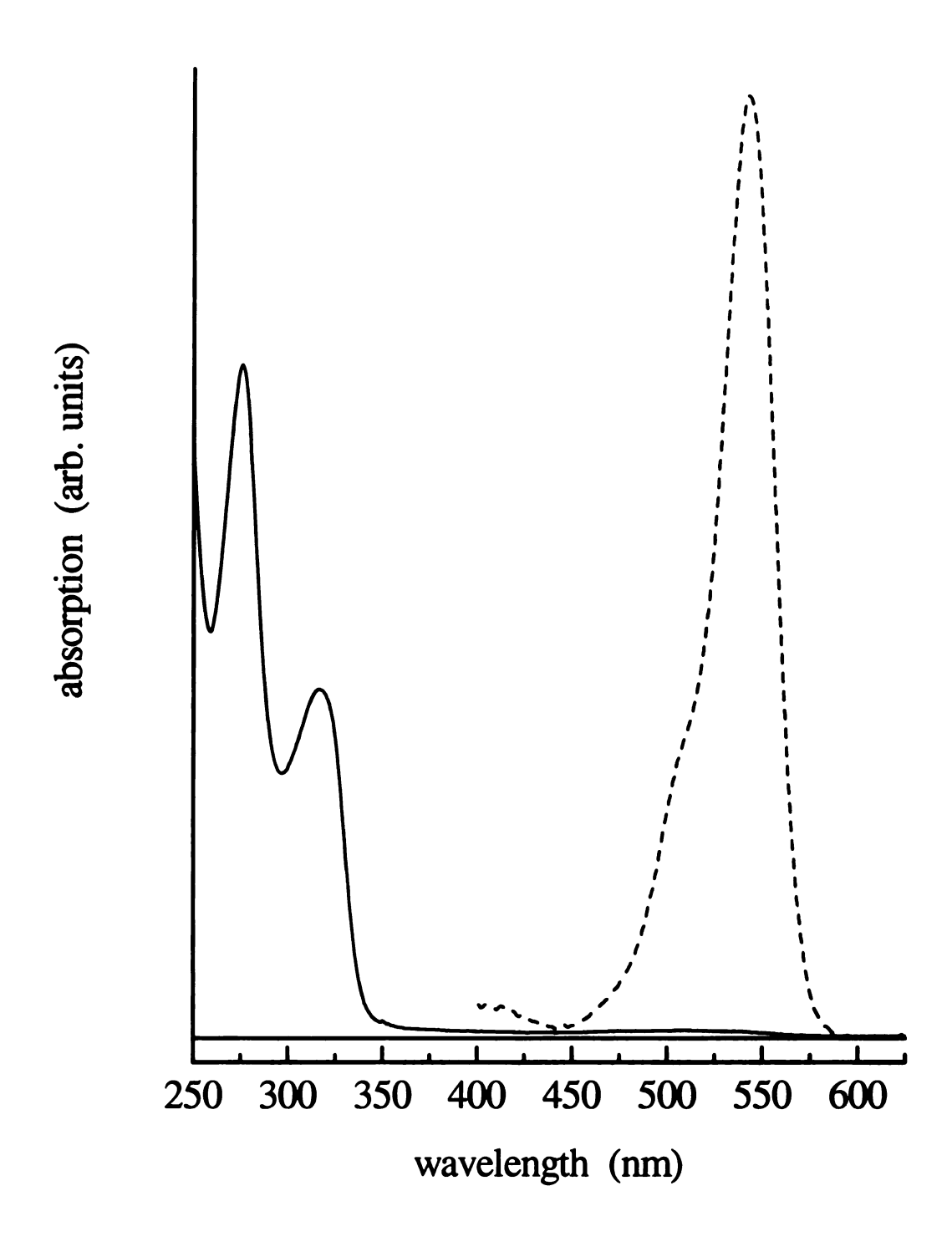


Figure 3.4 - Absorption spectra of R610 lactone (solid line) in acetonitrile and ring-opened R610 lactone (dashed line) in methanol.

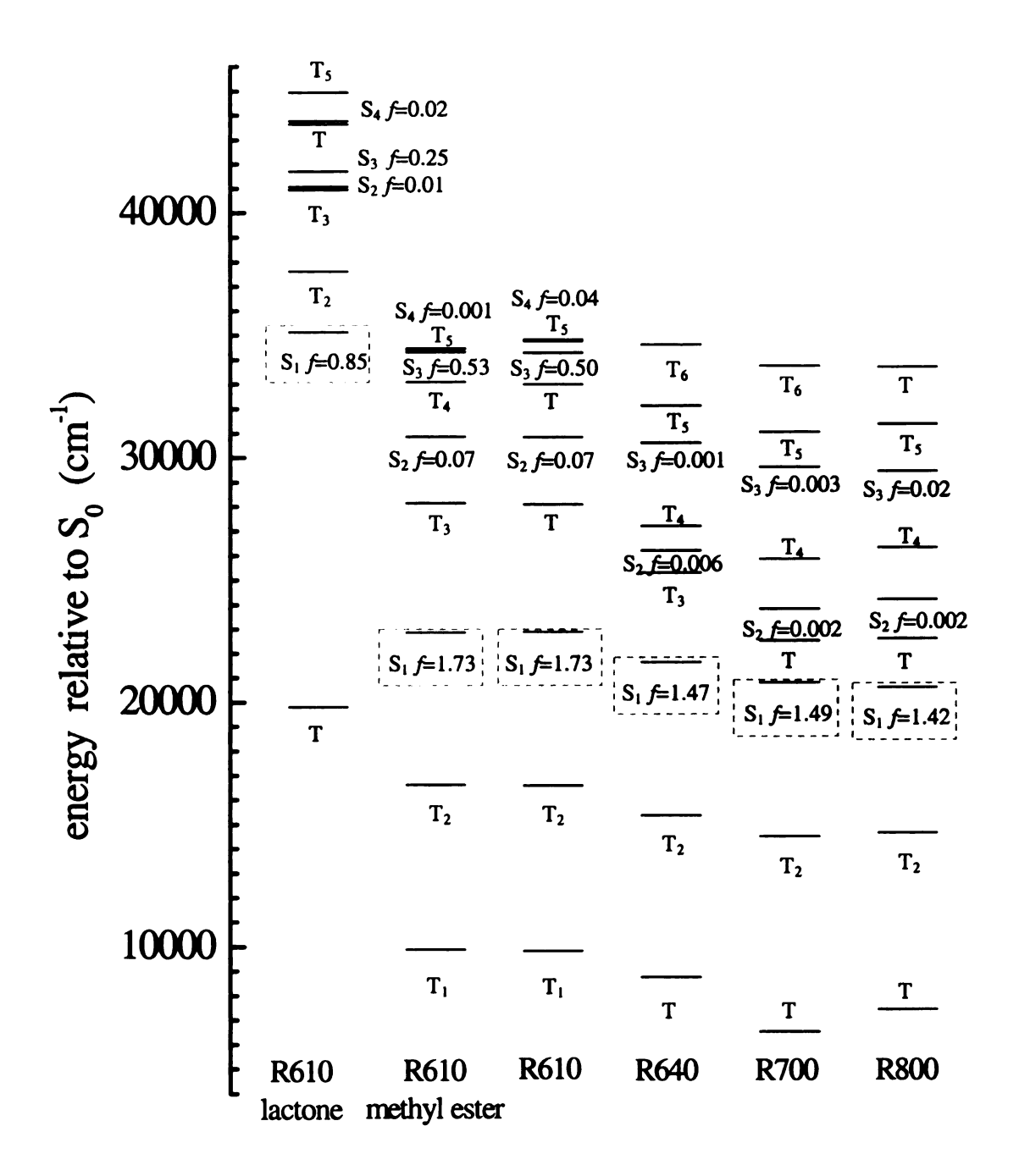


Figure 3.5 - Calculated state energy levels for the rhodamines studied here. Calculations were performed at the semi-empirical level with PM-3 parameterization. State energies and oscillator strengths for $S_n \leftarrow S_0$ transitions were calculated using configuration interaction.

For all data, the reported zero-time anisotropies are derived from the regression of the data for times greater than 15 ps after excitation, and the uncertainties reported for each quantity are 95 % confidence intervals for six or more individual determinations. We report the quantities R(0) and τ_{OR} in Table 3.1 for the several rhodamines and solvents used.

Table 3.1a. Reorientation Times and Zero-Time Anisotropies for R610, R640 and R610 lactone in

protic and aprotic solvents.

productand aprovide dorrondo						
	Rhodami	ne 610ª	Rhodamine 640 ^a		Ring-opened Rhodamine 610 lactone a, b	
Solvent	R(0)	$ au_{ m OR}$	R(0)	$ au_{ m OR}$	R(0)	$ au_{ m OR}$
Acetonitrile	0.26±0.02	57±3	0.25±0.05	50±3	-	-
Methanol	0.26±0.03	87±6	0.24±0.02	68±2	0.29±0.04	95±5
DMF	0.26±0.03	138±5	0.28±0.02	125±2	-	-
Water	0.23±0.03	141±6	0.24±0.06	121±3	0.2±0.01	129±10
Ethanol	0.29±0.03	143±4	0.25±0.02	135±6	0.22±0.01	154±9
n-Propanol	0.27±0.01	229±5	0.25±0.02	227±12	0.27±0.01	310±11
DMSO	0.32±0.03	271±15	0.24±0.04	264±18	-	-

The data are the best fit results of the data to the function $R(t) = R(0)\exp(-t/\tau_{OR})$. Time constants are in ps and the uncertainties are standard deviations $(\pm 1\sigma)$ for at least six determinations of each quantity.

Table 3.1b - Reorientation Times and Zero-Time Anisotropies for R700 and R800 in protic and aprotic solvents.

	Rhodamine 700 ^a		Rhodamine 800 ^a	
Solvent	R(0)	$ au_{ m OR}$	R(0)	$ au_{ m OR}$
Acetonitrile	0.20±0.01	42±1	0.22±0.02	47 ± 5
Methanol	0.17±0.02	48±4	0.22±0.02	50 ± 4
DMF	0.21±0.01	97±7	0.27±0.01	101 ± 7
Water	0.26±0.02	110±10	0.25±0.02	122 ± 11
Ethanol	0.23±0.01	89±3	0.24±0.04	94 ± 6
n-Propanol	0.19±0.02	152±6	0.22±0.04	156 ± 7
DMSO	0.26±0.03	213±15	0.24±0.02	217 ± 10

^a The data are the best fit results of the data to the function $R(t) = R(0)\exp(-t/\tau_{OR})$. Time constants are in ps and the uncertainties are standard deviations (±1 σ) for at least six determinations of each quantity.

The intermolecular interactions of most interest to us are between polar organic chromophores and associative solvents and systems that can exhibit spontaneous self-assembly phenomena. For such studies, some spectroscopic property of the

^b Some data for R610 lactone was not obtained. See text for explanation.

chromophore is monitored as a function of a systematic change in the system, such as viscosity or polarity.⁴⁹⁻⁵³ In many cases, collecting information in the time domain is most instructive, with orientational relaxation measurements being perhaps the most information-rich for our purposes.

Debye-Stokes-Einstein equation. The starting point for the interpretation of molecular reorientation measurements is usually the modified Debye-Stokes-Einstein (DSE) equation. 54-56

$$\tau_{OR} = \frac{\eta V f}{k_B T S} \tag{3.2}$$

This simple model has proven to be remarkably successful in providing at least a semiquantitative model for the rotational motion of molecules in solution. In this model, η is the solvent bulk viscosity, V is the solute hydrodynamic volume, ⁵⁷ and the terms f and Sare frictional boundary condition⁵⁶ and molecular shape factors, respectively.⁵⁵ The frictional boundary condition and molecular shape factors arise from modifications of the original theory, which described the reorientation of spheroidal particles in a microwave cavity. The DSE model assumes a continuum solvent and it has been shown to model reorientation data quantitatively in the limit that the individual solvent molecules are smaller than the solute. 43-45,51,58-68 Discrepancies between the modified DSE model and experimental data are often expressed in terms of the molecular-level breakdown of the notion of viscosity or in terms of variations in the friction coefficient, f, that are related to the interactions between solvent and solute molecules. The main limitation of the DSE model in the prediction of solute reorientation lies with the molecular-scale definition of the solute-solvent boundary condition. Indeed, this model treats the solvent as a continuum and is thus incapable of accounting for specific chemical interactions. For

solvent-solute interactions with a substantial frictional component, the so-called "stick limit" is used, $^{5,7,51,53,66,69-72}$ and for cases where frictional interactions are expected to be less significant, e.g. reorientation of nonpolar solutes in nonpolar solvents, the "slip" limit is used. In this limit, f can range in value from 0 to 1, with its exact value being determined by the effective shape of the volume swept out by the reorienting molecule. For some ionic solutes in polar solvents, the reorientation times measured experimentally exceed those predicted by the modified DSE equation in the stick limit, and such systems are termed "super-stick". The central issue for such systems is determining the dominant contribution(s) to the solvent-solute boundary condition, with dielectric friction 73 and hydrogen bonding 60,61 being proposed to account for the experimental data.

The data we present in this paper are predicted reasonably well by stick limit reorientation, save for one case. The ring-opened form of R610 lactone reorients more slowly than R610 and we understand this behavior based on the formation of an alkyl ester by reaction of the R610 lactone with the alcohol solvent (*vide infra*). We find that the reorientation of rhodamines in polar aprotic solvents is consistent with stick or slightly "super stick" limit behavior, while the reorientation of these same chromophores in alcohols is slightly sub-stick. We examine these data in terms of solvent-solute interactions and the internal structural freedom available to the chromophores, an effect which can influence the effective rotor shape of the reorienting moiety and, under some circumstances, can affect its apparent hydrodynamic volume.⁴⁷

Among the factors that can contribute to stick or super-stick reorientation behavior is dielectric friction.^{64,69,70,73-76} Dielectric friction impedes rotational motion of molecules in solution based on the strength of dipole-induced dipole interactions. The

fluctuations will couple to the solute permanent dipole moment, with the strength of coupling scaling as r⁻⁶. The interaction of the solvent fluctuations with the solute dipole moment induces a torque on the rotating molecule that acts to slow its motion. This contribution to the solvent-solute boundary condition is expected to operate in addition to the frictional terms considered in the DSE treatment, and several methods have been used to evaluate the contribution of dielectric friction to solute reorientation. 65,73,74,77 For the rhodamines and solvents we use here, this effect is found to be a minor factor relative to frictional interactions (see Table 3.2).

In protic solvents, both solvent-solvent and solvent-solute hydrogen bonding can play a significant role in mediating solute motion. The characteristic persistence time of these interactions in long-chain alkanols is similar to the reorientation times seen for polar solutes in the size range of the rhodamines.⁶⁰ Hydrogen bonding interactions are known to play a significant role in determining solvent bulk viscosity and the Blanchard group has reported previously on evidence for strong solvent-solute hydrogen bonding interactions in alcohols and their effect on the reorientation dynamics observed for these systems.^{43,60,61} In cases where H-bonding can play a role, the interaction is typically between the solvent alcohol proton and a specific functionality on the solute, such as an amine group. These interactions persist for sufficient time, on average, that the effect is to increase the hydrodynamic volume of the reorienting moiety (solute plus attached solvent), an effect that can be modeled effectively within the framework of the modified DSE equation.

Table 3.2. Calculated dielectric friction times for Rhodamine 610 (R610) and 640 (R640). The times reported are intended to be additive contributions to the reorientation time calculated using the modified DSE model.

Solvent	R610 (ps) ^a	R640 (ps) ^a	
Acetonitrile	0.1	0.1	
Methanol	0.9	0.8	
DMF	0.4	0.3	
Water	0.1	0.0	
Ethanol	2.2	2.1	
n-Propanol	10.9	10.2	
DMSO	0.2	0.2	

^a Values are calculated from Nee and Zwanzig, reference 73. Some values necessary for completion of the calculation are taken from Table 3.4 and references contained therein.

Reorientation of R610, R640 and R610 lactone. We show the solvent viscositydependence of R610 and R640 reorientation in Figure 3.6, along with the dependence predicted from Eq. 3.2 (lines). The data show that, with minor exceptions, both R610 and R640 reorient in the DSE stick limit, for both polar protic and aprotic solvents. Using the finding that the rhodamines reorient as prolate rotors, we calculate a shape factor of S = 0.9 for both R610 and R640 using Perrin's equations. 55,56 The reorientation dynamics of these two rhodamines are expected to be similar based on their hydrodynamic volumes, 418 Å³ for R610 and 443 Å³ for R640 (see Table 3.3).⁵⁷ It is well established that polar solutes such as rhodamines reorient more slowly in polar protic solvents than the DSE model would predict while in polar aprotic solvents, they are modeled well by the (modified) DSE equation. 50,58,66-68 This trend can be understood to a significant extent based on the characteristic persistence time of solvent-solute interactions. This interaction time has been shown to correlate with the longitudinal relaxation time, τ_L , of the solvent, at least for polar aprotics. 1-3,62 The longitudinal relaxation times for the solvents used here (τ_L , Table 3.4) show that the dielectric relaxation times for the low

viscosity protic and aprotic solvents are very similar and all are fast on the timescale of reorientation.

Table 3.3. Calculated molecular volumes and S0 permanent dipole moments for the rhodamines examined here. Volumes were calculated from Reference 57. Dipole moments were calculated using Hyperchem® v. 6.0 with PM-3 parameterization.

Probe	Volume (Å ³)	μ (D)	
R610	418	2.7	
R640	443	2.6	
R610 lactone	415	6.7	
R700	375	5.7	
R800	364	3.7	

Thus, the results for this system are substantially in keeping with the DSE model and there is little distinction between reorientation in polar protic and aprotic solvents because the reorientation time constants for the two chromophores are much longer than the longitudinal relaxation times for the solvents studied. Figure 3.4 shows the absorption spectra of both the lactone and ring-opened forms of R610 lactone. R610 lactone undergoes a ring-opening reaction in alcohols to form the alkyl ester of R610. This reaction does not proceed in polar aprotic solvents and the reorientation data are available only for the ring-opened R610 lactone only in alcohols. We show these data in Figure 3.7, along with the reorientation data for R610 for comparison. The reorientation of the ring-opened R610 lactone and R610 are measurably different and we ascribe this difference to the added volume of the alkyl ester. We note that the addition of the aliphatic tail to the R610 chromophore yields reorientation behavior that is consistent with the "super-stick" limit. We believe that this phenomenon is the result of relatively strong interactions between the (alkyl) ester functionality and the solvent. This argument is equivalent to the assertion that the interactions between the R610 aliphatic ester moiety

and the surrounding solvent is of the same order as solvent-solvent interactions that give rise to the relatively high viscosity of the alkanols.

Table 3.4. Selected properties for the solvents used.

Solvent	Viscosity (cP)	Volume (ų)	μ (D)	τ_{D}^{a} (ps)	n	ε ₀	τ _L ^b (ps)
Acetonitrile	0.369	47.1	3.92	3.9	1.34	37.5	0.2
Methanol	0.544	36.1	1.70	55.6	1.328	32.6	3.0
DMF	0.794	76.6	3.82	27.4	1.43	36.7	1.5
Water	0.89	20.6	1.85	8.2	1.333	78.5	0.2
Ethanol	1.074	53.1	1.69	105	1.361	24.3	8.0
n-Propanol	1.945	70.1	1.68	435	1.386	20.1	41.6
DMSO	1.987	76.8	3.96	20.6	1.478	4.7	9.6

^a Values for τ_D are from reference 45. Blanchard, G. J. J. Chem. Phys. 1991, 95, 6317-6325. and references therein. Volumes are calculated from reference 50. Tao, T. Biopolymers 1969, 8, 609-632. Viscosity values are from references 60. Blanchard, G. J. J. Phys. Chem. 1988, 92, 6303-6307. and 78. Handbook of Chemistry and Physics; 82 ed.; Lide, D. R., Ed.; CRC Press: Boca Raton, 2001. Solvent dipole moments (vapor phase) are taken from reference 78. Handbook of Chemistry and Physics; 82 ed.; Lide, D. R., Ed.; CRC Press: Boca Raton, 2001.

b $\tau_1 = (\epsilon_m/\epsilon_0)\tau_{D_0} \epsilon_m = n^2$

Reorientation of 700 and R800. The reorientation dynamics of R700 and R800 are shown in Figure 3.8 as a function of solvent viscosity, along with the DSE predictions. Included with the data are two lines, the upper being the DSE predicted reorientation in the "stick" limit and the lower the DSE predicted "slip" limit. These values of the boundary conditions were obtained using the "stick" limit (f = 1) or the calculated "slip" limit ($f \sim 0.1$) for a prolate rotor with shape factors S = 0.81 (R700) and 0.84 (R800). The shape factor was calculated according to Perrin and the slip limit frictional term was determined using the method of Hu and Zwanzig. The reorientation data for these two molecules show a clear distinction between polar protic and aprotic solvents.

In the solvents methanol, ethanol and propanol, both R700 and R800 exhibit slightly substick reorientation times while in water and the polar aprotic solvents, we observe stick-limit behavior. The reorientation dynamics measured in the alcohols are not consistent

with slip-limit predictions, but there are two clearly discernible groups of data (Figure 3.8). The data for R610 and R640 reorientation differ qualitatively from that seen for R700 and R800. For the first two chromophores, there is not a clear distinction between their reorientation dynamics in polar protic and aprotic solvents, while there is clear distinction for R700 and R800. It is tempting to ascribe this difference in behavior to differences in the structures of these two groups of molecules, and, indeed, several distinctions can be made based on structure. The first distinction is that the calculated permanent ground state dipole moments of R610 and R640 are smaller than those for R700 and R800 (Table 3.3). This finding is consistent with the experimental data in the sense that, for R610 and R640, we observe little discernible difference between their reorientation behavior in the alcohols and in polar aprotic solvents. For R700 and R800, we observe stronger solvent-solute interactions for polar aprotic solvents than for the alcohols or water. The larger permanent dipole moment of these two chromophores serves to interact with solvents characterized by large permanent dipole moments (Table 3.4). Another structural feature that is worthy of examination is the shape of the chromophores. R610 and R640, by virtue of their o-benzoate group at the 1 position, are expected to sweep out volumes that are substantially more spherical than that seen for R700 and R800. This effect is seen in the calculated shape factors for these two groups of molecules; $S \sim 0.9$ for R610 and R640 and $S \sim 0.8$ for R700 and R800. In the stick limit, such a distinction would not matter, but in the slip limit, the frictional term f would be larger for R700 and R800 than for R610 and R640. We are not implying that the rhodamines behave in the slip limit for the solvents we have studied here, but if there is any slip-like component to frictional solvent-solute interactions, we assert that such

contributions would be more prominent in systems with a more anisotropic rotor shape, hence the more pronounced solvent dependence for R700 and R800. In comparing the reorientation dynamics of R610 and R640, we would expect R610 to be slightly faster than R640 on the basis of the (small) difference in hydrodynamic volume. Instead, we find that R610 exhibits reorientation times equal to or longer than those of R640 in all of the solvents studied. This effect is especially pronounced in the solvents water, methanol and ethanol (Table 3.1). We understand this behavior in terms of the motional freedom of the terminal amines in R610 and their restricted motion in R640. Semi-empirical calculations show that when free to rotate, the amino groups are capable of stabilizing a partial positive charge, making them more amenable to strong solvent-solute interactions. When both dipolar and structural contributions to the reorientation and linear response of the rhodamines are considered, we can understand the behavior of these chromophores within the framework of a single system.

Conclusions

We have examined the linear optical response and reorientation dynamics of several rhodamines in a series of polar protic and aprotic solvents. The reorientation data are all qualitatively consistent with the modified DSE model in the stick limit. At a quantitative level, several trends emerge. The first is that dipolar solvent-solute interactions are at least as important in determining reorientation dynamics as are H-bonding interactions for the rhodamines, and the distinction between polar protic and aprotic solvents is most clear for rhodamines with small polar substituents at the 1 position. We also find that H-bonding interactions with the chromophore terminal amino groups are more prominent in chromophores where the amino groups are free to rotate,

and we understand this phenomenon in the context of the ability of the free and locked amino groups to stabilize charge. In the case of reactive systems, such as R610 lactone, only polar protic solvents are capable of participating in a lactone ring-opening reaction to form an ester. Our reorientation data reflect the formation of the ester and, for the esters, we observe stronger solvent-solute interactions than are seen for the native chromophore, R610. The basis for this finding requires further investigation.

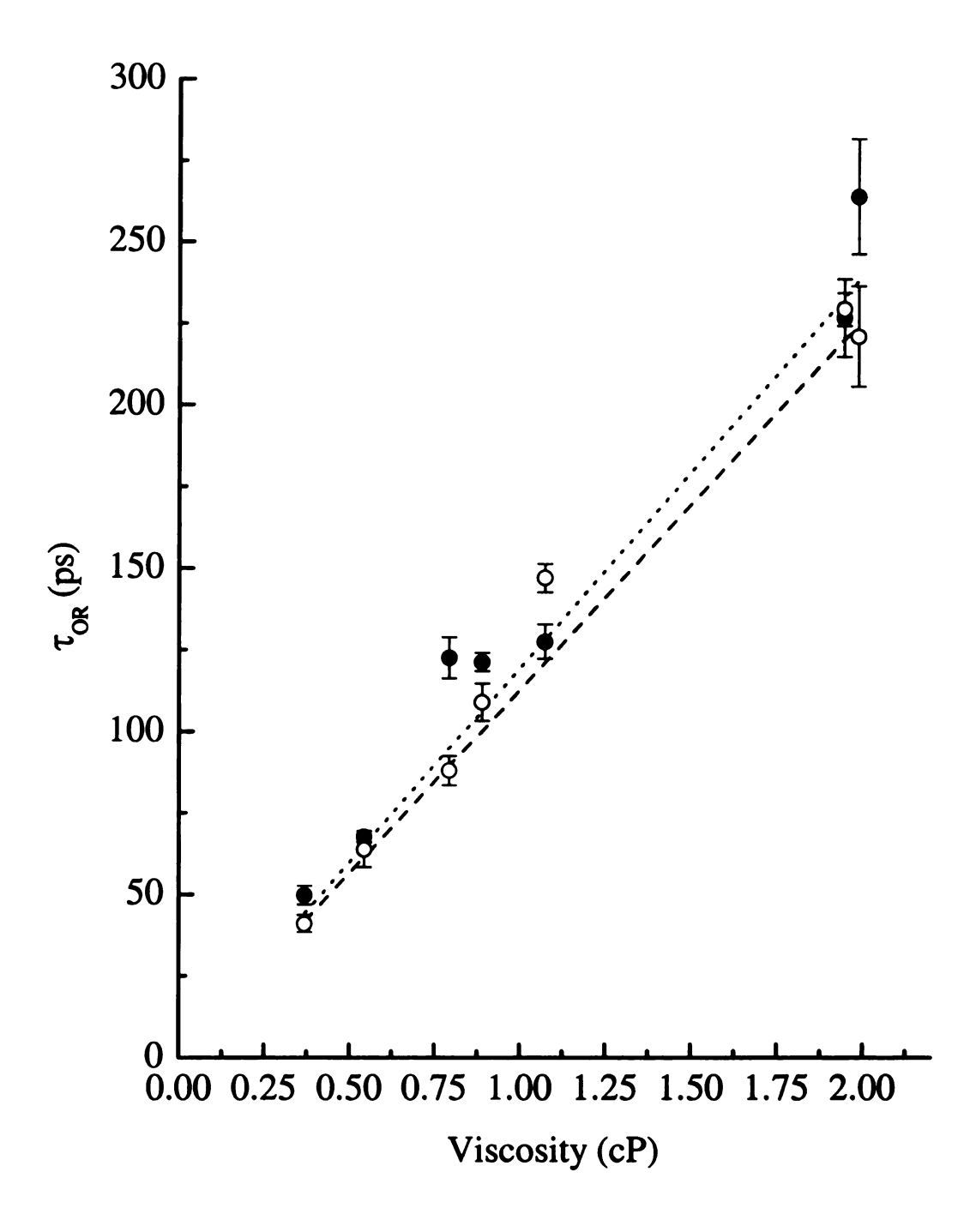


Figure 3.6 - Reorientation time constants of R610 (•) and R640 (•) as a function of solvent viscosity. The calculated DSE stick limit line is shown for each chromophore, with a dashed line for R610 and a dotted line for R610.

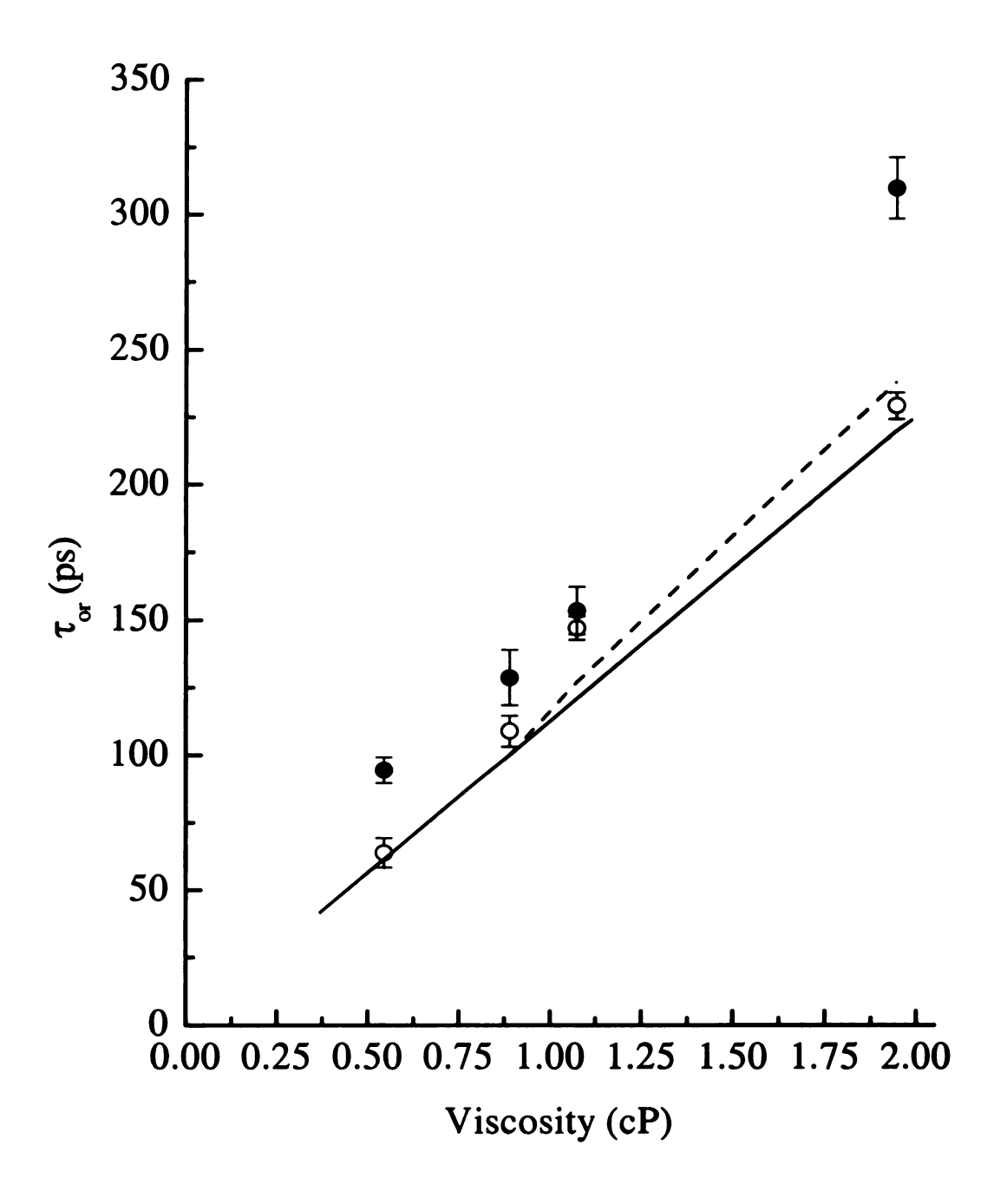


Figure 3.7 - Reorientation time constants of ring-opened R610 lactone (•) and R610 (o) as a function of solvent viscosity. The calculated DSE stick limit lines are shown for each chromophore. For the ring-opened lactone, the calculated hydrodynamic volume reflects an increase due to ester formation.

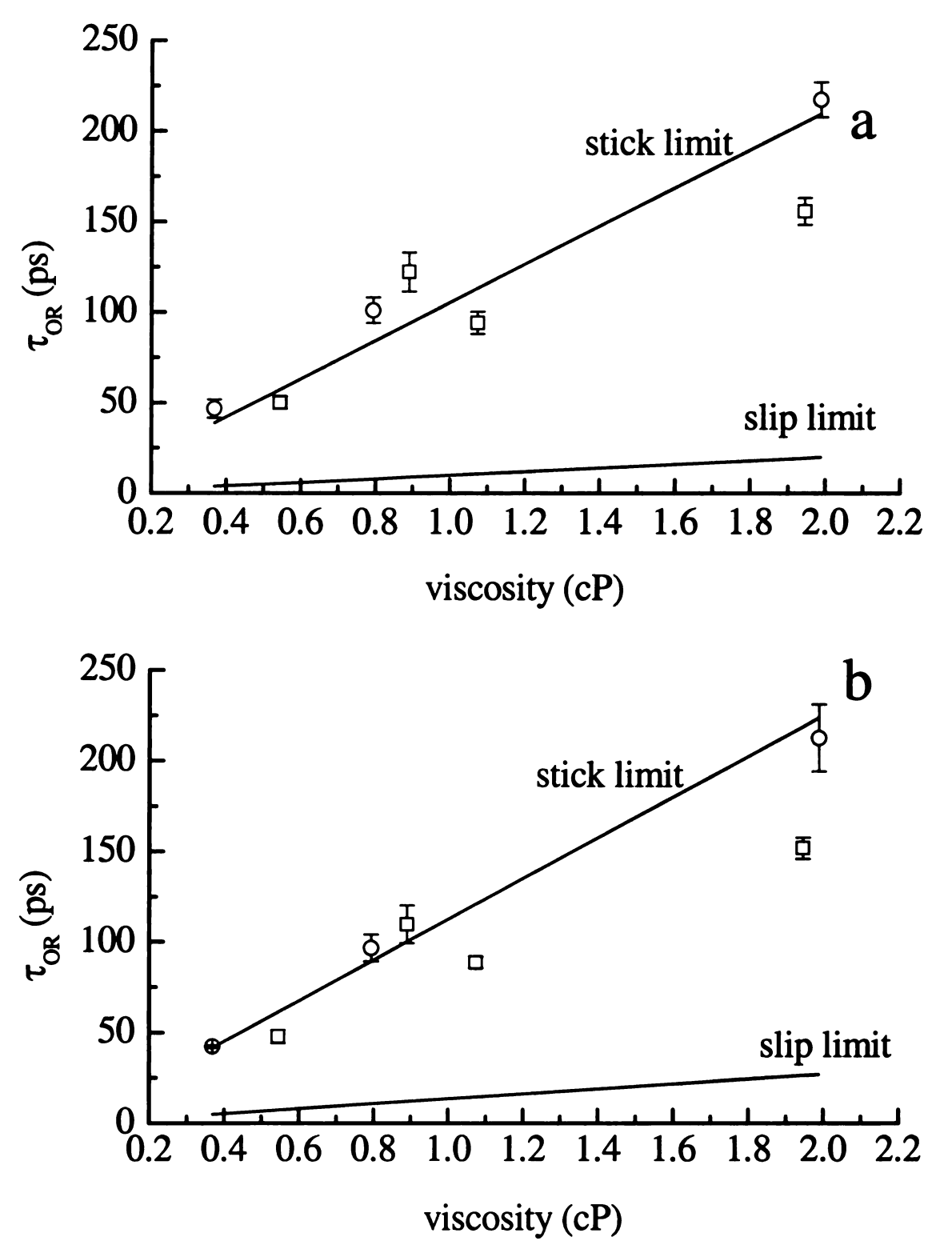


Figure 3.8 - Reorientation time constants of (a) R700 and (b) R800 as a function of solvent viscosity. Aprotic solvents are shown with open (\circ) circles and protic solvents are shown with open (\circ) squares. For each chromophore the calculated DSE stick and slip limit lines are shown.

Literature Cited

- (1) Maroncelli, M.; Fleming, G. R. J. Chem. Phys. 1990, 92, 3251.
- (2) Maroncelli, M.; Fleming, G. R. J. Chem. Phys. 1987, 86, 6221.
- (3) Yip, R. W.; Wen, Y.-X.; Szabo, A. G. J. Phys. Chem. 1993, 97, 10458.
- (4) Su, S.; Simon, J. D. J. Phys. Chem. 1989, 93, 753.
- (5) Simon, J. D. Acc. Chem. Res. 1988, 21, 128.
- (6) Kahlow, M. A.; Jarzeba, W.; Kang, T. J.; Barbara, P. F. J. Chem. Phys. 1989, 90, 151.
- (7) Kahlow, M. A.; Kang, T. J.; Barbara, P. F. J. Chem. Phys. 1988, 88, 2372.
- (8) Su, S.; Simon, J. D. J. Phys. Chem. 1987, 91, 2693.
- (9) Declemy, A.; Rulliere, C.; Kottis, P. Chem. Phys. Lett. 1987, 133, 448.
- (10) Chapman, C. F.; Fee, R. S.; Maroncelli, M. J. Phys. Chem. 1990, 94, 4929.
- (11) Ittah, V.; Huppert, D. Chem. Phys. Lett. 1990, 173, 496.
- (12). Kohn, F.; Hofkens, J.; De Schryver, F. C. Chem. Phys. Lett. 2000, 321, 372.
- (13) Johnson, L. V.; Walsh, M. L.; Chen, L. B. *Proc. Natl. Acad. Sci., USA* 1980, 77, 990.
- (14) Renge, I. J. Phys. Chem. A 2001, 105, 9094.
- (15) Ghanadzadeh, A.; Zanjanchi, M. A. Spectrochim. Acta, Part A 2001, 57, 1865.
- (16) Pevenage, D.; Van der Auweraer, M.; De Schryver, F. C. Langmuir 1999, 15, 8465.
- (17) Becker, S.; Gregor, I.; Theil, E. Chem. Phys. Lett. 1998, 283, 350.
- (18) Beaumont, P. C.; Johnson, D. G.; Parsons, B. J. J. Photochem. Photobiol., A 1997, 107, 175.
- (19) Menzel, R.; Theil, E. J. Phys. Chem. A 1998, 102, 10916.
- (20) Watarai, H.; Funaki, F. Langmuir 1996, 12, 6717.

- (21) Preininger, C.; Mohr, G. J.; Klimant, I.; Wolfbeis, O. S. Anal. Chim. Acta 1996, 334, 113.
- (22) Drexhage, K. H. In *Dye Lasers*; 2nd ed.; Schaefer, F. P., Ed.; Springer: Berlin, 1977; pp 144.
- (23) Jiang, Y.; Hambir, S. A.; Blanchard, G. J. Opt. Commun. 1993, 99, 216.
- (24) Blanchard, G. J.; Wirth, M. J. Anal. Chem. 1986, 58, 532.
- (25) Andor, L.; Lorincz, A.; Siemion, J.; Smith, D. D.; Rice, S. A. Rev. Sci. Instrum. 1984, 55, 64.
- (26) Bado, P.; Wilson, S. B.; Wilson, K. R. Rev. Sci. Instrum. 1982, 53, 706.
- (27) Stewart, J. J. P. J. Comp. Chem. 1989, 10, 221.
- (28) Stewart, J. J. P. J. Comp. Chem. 1989, 10, 209.
- (29) Dewar, M. J. S.; Thiel, W. J. Am. Chem. Soc. 1977, 99, 4899.
- (30) Dewar, M. J. S.; Thiel, W. J. Am. Chem. Soc. 1977, 99, 4907.
- (31) Suvorov, B. A. Russ. J. Org. Chem. 1998, 34, 994.
- (32) Sheppard, W. A. J. Am. Chem. Soc. 1965, 87, 2410.
- (33) Roberts, J. D.; Webb, R. L.; McElhill, E. A. J. Am. Chem. Soc. 1950, 72, 408.
- (34) Ramette, R. W.; Sandell, E. B. J. Am. Chem. Soc. 1956, 78, 4872.
- (35) Klein, U. K. A.; Hafner, F. W. Chem. Phys. Lett. 1976, 43, 141.
- (36) Sadkowski, P. J.; Fleming, G. R. Chem. Phys. Lett. 1978, 57, 526.
- (37) Rosenthal, I.; Peretz, P.; Muszkat, K. A. J. Phys. Chem. 1979, 83, 350.
- (38) Snare, M. J.; Treloar, F. E.; Ghiggino, K. P.; Thistlethwaite, P. J. J. Photochem. 1982, 18, 335.
- (39) Selwyn, J. E.; Steinfeld, J. I. J. Phys. Chem. 1972, 76, 762.
- (40) Ferguson, J.; Mau, A. W. H. Chem. Phys. Lett. 1972, 17, 543.
- (41) Hinckley, D. A.; Seybold, P. G.; Borris, D. P. Spectrochim. Acta, Part A 1986, 42, 747.

- (42) Hinckley, D. A.; Seybold, P. G. Spectrochim. Acta, Part A 1988, 44, 1053.
- (43) DelaCruz, J. L.; Blanchard, G. J. J. Phys. Chem. A 2001, 105, 9328.
- (44) Blanchard, G. J. J. Phys. Chem. 1991, 95, 5293.
- (45) Blanchard, G. J. J. Chem. Phys. 1991, 95, 6317.
- (46) Rasimas, J. P.; Berglund, K. A.; Blanchard, G. J. J. Phys. Chem. 1996, 100, 17034.
- (47) Rasimas, J. P.; Berglund, K. A.; Blanchard, G. J. J. Phys. Chem. 1996, 100, 7220.
- (48) Rasimas, J. P.; Blanchard, G. J. J. Phys. Chem. 1996, 100, 11526.
- (49) Favro, D. L. Phys. Rev. 1960, 119, 53.
- (50) Tao, T. Biopolymers 1969, 8, 609.
- (51) Chuang, T. J.; Eisenthal, K. B. J. Chem. Phys. 1972, 57, 5094.
- (52) Porter, G.; Sadkowski, P. J.; Tredwell, C. J. Chem. Phys. Lett. 1977, 49, 416.
- (53) Spears, K. G.; Cramer, L. E. Chem Phys. 1978, 30, 1.
- (54) Debye, P. Polar Molecules Chemical Catalog Co.: New York 1929.
- (55) Perrin, F. J. Phys. Radium 1934 5, 497.
- (56) Hu, C.; Zwanzig, R. J. Chem. Phys. 1974, 60, 4354.
- (57) Edward, J. T. J. Chem Ed. 1970, 47, 261.
- (58) Fleming, G. R.; Morris, J. M.; Robinson, G. W. Chem. Phys. 1976, 17, 91.
- (59) Blanchard, G. J. J. Chem. Phys. 1987, 87, 6802.
- (60) Blanchard, G. J. J. Phys. Chem. 1988, 92, 6303.
- (61) Blanchard, G. J.; Cihal, C. A. J. Phys. Chem. 1988, 92, 5950.
- (62) Horng, M.-L.; Gardecki, J. A.; Maroncelli, M. J. Phys. Chem. A 1997, 101, 1030.
- (63) Balabai, N.; Kurnikova, M. G.; Coalson, R. D.; Waldeck, D. H. J. Am. Chem. Soc. 1998, 120, 7944.

- (64) Wiemers, K.; Kauffman, J. F. J. Phys. Chem. A 2000, 104, 451.
- (65) Waldeck, D. H. The Role of Solute-Solvent Friction in Large-Amplitude Motions. In *Conformational Analysis of Molecules in Excited States*; Waluk, J., Ed.; Wiley-VCH, 2000; pp 113-176.
- (66) von Jena, A.; Lessing, H. E. Chem. Phys. Lett. 1981, 78, 187.
- (67) von Jena, A.; Lessing, H. E. Chem. Phys. 1979, 40, 245.
- (68) von Jena, A.; Lessing, H. E. Ber. Bunsen-Ges. Phys. Chem. 1979, 83, 181.
- (69) Madden, P.; Kivelson, D. J. Phys. Chem. 1982, 86, 4244.
- (70) Philips, L. A.; Webb, S. P.; Clark, J. H. J. Chem. Phys. 1985, 83, 5810.
- (71) Philips, L. A.; Webb, S. P.; Yeh, S. W.; Clark, J. H. J. Phys. Chem. 1985, 89, 17.
- (72) Kahlow, M. A.; Kang, T. J.; Barbara, P. F. J. Phys. Chem. 1987, 91, 6452.
- (73) Nee, T.-W.; Zwanzig, R. J. Chem. Phys. 1970, 52, 6353.
- (74) Alavi, D. S.; Waldeck, D. H. J. Chem. Phys. 1991, 94, 6196.
- (75) Kivelson, D.; Spears, K. G. J. Phys. Chem. 1985, 89, 1999.
- (76) Ladanyi, B. M.; Stratt, R. M. J. Chem. Phys. 1999, 111, 2008.
- (77) Alavi, D. S.; Hartman, R. S.; Waldeck, D. H. J. Chem. Phys. 1991, 95, 6770.
- (78) Handbook of Chemistry and Physics; 82 ed.; Lide, D. R., Ed.; CRC Press: Boca Raton, 2001.

Chapter 4.

Dynamics of Rhodamine Esters in Micellar Media: Probing the Balance Between Ionic and Dispersion Interactions

Introduction

Amphiphilic systems are important to a number of chemical processes ranging from the existence of lipid bilayers to the use of detergents in industrial and home applications. The single feature of such systems that allows such broad utility is their ability to coexist with and function as an interface between polar and nonpolar phases. This ability is determined by a balance between ionic and dipolar interactions with polar media and dispersion interactions with nonpolar media. Micelles are a subset of amphiphilic systems that manifest transient self-assembly behavior in certain concentration regimes, and this family of solution-phase assemblies has been studied extensively.

Micelles have attracted significant attention because of their ability to function as encapsulating and/or biomimetic systems. Among the properties of micelles that have been investigated are the effects of amphiphile concentration on size, shape and permeability, and time-domain optical spectroscopy has emerged as a very useful tool for such studies. Many dynamical studies of micelles have focused on associating a probe molecule with the micellar environment and correlating the observed dynamics of the probe molecule with that of the micelle as a function of pressure, viscosity and probe solubility. 1-19

Despite the widely held understanding that the formation and existence of micelles represents a balance between dispersion and ionic or dipolar intermolecular interactions, a detailed understanding of this balance remains to be articulated. The approach taken to understanding the behavior of micellar systems has been to use an optical probe that exhibits limited solubility in both the micelle and the aqueous phases, with the dynamical response of the system modeled in the context of the simultaneous observation of the same chromophore in multiple environments. A motivation for interpreting dynamical data within this framework has been the observation of biexponential induced orientational anisotropy decays, with the assumption that the chromophore in each environment is characterized by a single exponential anisotropy decay. These multicomponent anisotropy decay data could be interpreted either as evidence for lateral diffusion into and out of the micelles or as reorientation of chromophores partitioned into two distinct environments. Save for systems designed to force the chromophore into one environment or the other, chromophores will establish a dynamic equilibrium between the two phases and a significant issue in understanding such data is the time scale of dynamic exchange relative to the time scale of the reorientation measurements.

For many systems, it makes sense to consider the average environment of the chromophore. We expect that the environment of a micelle will vary in a regular manner as a function of distance from the center of the micelle, going from a relatively dense aliphatic environment near the center to a relatively diffuse region known as either the Stern layer in charged micelles, or as the Palisade layer in neutral micelles, ²⁰⁻²² where the head groups, counter-ions and solvent molecules coexist. Several groups have performed

studies using chromophores that were not water soluble, but were soluble in the aliphatic portions of the micelle, and recovered the result that these chromophores "partitioned" between the different regions within the micelle, a result consistent with the work of several other groups. ^{3,4,7,8,12,19,23} In systems where the probe chromophore is bound to some specific location on an amphiphile, which presumably retains its ability to participate in micelle formation, the chromophore is seen to exhibit a biexponential anisotropy decay, and this finding has been modeled in the context of the probe "wobbling" in a confined space. From these bodies of work, it is clear that the balance between ionic/polar and dispersion interactions is such that micelles are highly dynamic entities with the dynamics mediated by the details of the intermolecular interactions within and around the micelles. We are interested in exploring the structural factors that can influence this balance of forces. To elucidate these factors, we have performed rotational diffusion measurements using four rhodamine derivatives with varying aliphatic ester chain lengths. These are tetramethylrhodamine-methyl ester (R1), tetramethylrhodamine-ethyl ester (R2), tetraethylrhodamine-hexyl ester (R6) and tetraethylrhodamine-octadecyl ester (R18) (Figure 4.1), in three different aqueous micellar environments: cetyltrimethylamonium-bromide (CTAB), sodium dodecylsulfate (SDS) and polyethylene glycol 400 dodecyl ether (Thesit®) (Figure 4.1). The rhodamines are a family of robust chromophores that have found wide use as optical probes. These cationic dyes are water soluble and are thus good candidates for studies of micellar systems. Our data point to the expected partitioning between aqueous and micellar phases, with the details of the partitioning depending sensitively on the identity of the micelle head groups and the probe aliphatic chain length. We find that, for Thesit[®], the

rhodamine hexyl ester partitions into the micellar phase with anomalous efficiency, suggesting the importance of geometric issues related to the efficiency of probe-micelle interactions.

Experimental Section

Pump-Probe Laser System. The picosecond pump-probe laser spectrometer used to acquire reorientation data on the chromophores in water has been described in detail previously,²⁴ and we present only a brief synopsis of its operation here. A mode-locked CW Nd: YAG laser (Coherent Antares 76-S) produces 30 W of average power (1064 nm, 100 ps pulses, 76 MHz repetition rate). The output of this laser is frequency-doubled to produce ~3 W of average power at 532 nm, with the same pulse duration and repetition rate. The second harmonic light is used to excite two cavity-dumped dye lasers (Coherent 702-3) synchronously, with the output of both lasers being ~110 mW average power at 8 MHz repetition rate, producing ~7 ps fwhm autocorrelation traces using a three plate birefringent filter. The pump dye laser was operated using Pyromethine 567 dye (Exciton) at 556 nm and the probe laser was operated with Rhodamine 6G dye (Kodak) at 580 nm. The pump and probe wavelengths were chosen to access the $S_1 \leftarrow$ S₀ transition of each chromophore to detect the stimulated emission from each probe. The probe laser polarization was set alternately to 0° and 90° relative to the pump laser polarization for individual time-domain scans of parallel ($I_{\parallel}(t)$) and perpendicular ($I_{\perp}(t)$) polarization used in constructing the orientational anisotropy function. The time resolution of this system, ~10 ps, is determined by the cross-correlation of the pump and probe laser pulses. Detection of the transient signals was accomplished using a radioand audio-frequency triple-modulation scheme, with synchronous demodulation

detection. The reorientation time constants we report here are the average of 6 individual determinations, each comprised of the average of 10 - 12 sets of $I_{\parallel}(t)$ and $I_{\perp}(t)$ scans.

Time-correlated single photon counting spectroscopy. Rotational diffusion measurements of the probes in micellar systems were made using a spectrometer that has been described previously,²⁴ and we provide a synopsis of its essential features here. The source laser is a mode-locked CW Nd:YAG laser (Quantronix 416) producing 7 W average power at 1064 nm with 100 ps pulses at 80 MHz repetition rate. The second harmonic of the output of this laser (532 nm, ~700 mW) is used to excite a synchronously pumped, cavity dumped dye laser (Coherent 702-2) operating with Pyromethine 567 dye (Exciton) at 556 nm. The output of this laser is typically 100 mW average power with a 4 MHz repetition rate and 5 ps pulses. Detection of the transient fluorescence signals was accomplished using a microchannel plate photomultiplier tube (Hamamatsu R3809U), with fluorescence light collection through a reflecting microscope objective and wavelength selection with a subtractive double monochromator (American Holographics DB-10). The electronics used for signal processing are a Tennelec 455 quad constant fraction discriminator and a Tennelec 864 time-to-amplitude converter and biased amplifier. The reference channel was detected and delayed using an in-house built fiber optic delay line. Signals are processed using a multichannel analyzer (PCA Multiport II) and sent to a PC for acquisition. For this system, the instrument response function is typically 30 – 35 ps fwhm.

Steady-Sate Spectroscopy. The steady-state absorption spectra of the chromophores used here were recorded with 1 nm resolution using a Cary model 300

UV-visible spectrophotometer. The spontaneous emission spectra for the same solutions were obtained with 1 nm resolution using a SPEX Fluorlog-3 spectrometer.

Chemicals and Sample Handling. The probe molecules tetramethylrhodaminemethyl ester (R1), tetramethylrhodamine-ethyl ester (R2), tetraethylrhodamine-hexyl ester (R6), and tetraethylrhodamine-octadecyl ester (R18) (Figure 4.1) were obtained from Molecular Probes Inc. and used as received. Distilled, deionized water was available in-house. The chromophore concentration of all solutions used for laser measurements was 10 μ M. Measurements of R18 solutions in neat water were hampered by bleaching of the solution. This effect was mitigated by replacement with fresh solution on at least a daily basis, or as warranted. All pump-probe measurements were taken using a flowcell with a 1 mm pathlength, and TCSPC data were acquired using a fluorescence cuvette with a 1 cm path length. Solution temperatures were maintained at 298 \pm 0.5 K (Neslab EX100-DD).

The surfactants sodium dodecyl sulfate (SDS), cetyltrimethylammonium bromide (CTAB) and polyethylene glycol 400 dodecyl ether (Thesit[®]) (Figure 4.1) were obtained from Sigma-Aldrich, Inc., checked for fluorescent impurities, and used as received.

Results and Discussion

We are interested in using rhodamine alkyl esters as probes of micellar behavior.

Previous studies of rhodamines have provided a substantial understanding of their optical properties and the relationship(s) between chromophore structure and intermolecular interactions. Using this knowledge, we consider how to interrogate the balance of forces that give rise to micellar structures in aqueous amphiphile solutions. We have selected a series of rhodamine aliphatic esters with the idea that the ester aliphatic tails

will interact preferentially with the interior of the micelle and the cationic rhodamine chromophore will interact primarily with the micelle head groups. For anionic SDS micelles we expect attractive ionic interactions between chromophore and micelle head group and for cationic micelles we expect repulsive interactions. For this group of systems, the extent to which the chromophores partition into the micelles should depend sensitively on the chromophore aliphatic chain length. For neutral Thesit® micelles it is not clear whether attractive or repulsive polar interactions will dominate. To evaluate whether or not these expectations are realistic, we have examined the steady state spectroscopy and reorientation behavior of the Rhodamine esters in water and aqueous micellar media.

Linear optical response. The normalized absorption and emission spectra of the chromophores studied here are shown in Figure 4.2. With the exception of R6, the absorption and emission spectra of all the chromophores are not influenced by increasing the length of the ester chain. R6 exhibits a slight red-shift of ~ 7 nm in its absorption and emission spectra. Drexhage has studied the structure-spectroscopy relationships for rhodamines,³³ and his work has shown that the o-benzoate ring at the 1 position of these chromophores (Figure 1) is essentially decoupled from the three ring chromophore system, precluding a direct electronic effect from being responsible for the spectral shift we observe for R6. It is well established that substituents at the 4 and 12 positions do influence the spectral profiles of the rhodamines, and interactions between the ester aliphatic chain and the protons at the 4 and/or 12 positions could, in principle, account for our findings.

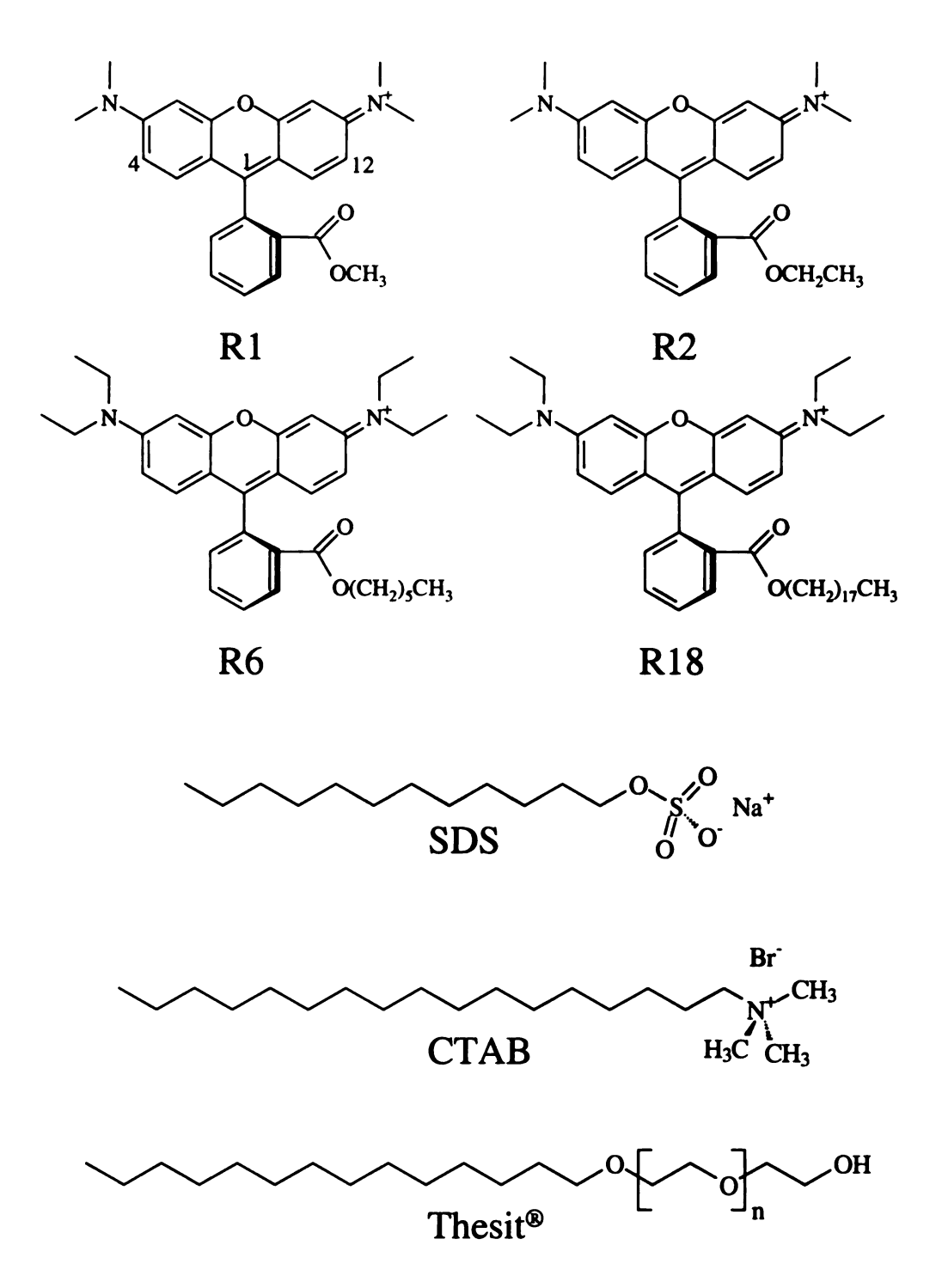


Figure 4.1 – Rhodamines and surfactants used in this study. Top row, left to right: tetramethylrhodamine methyl ester (R1), tetramethylrhodamine ethyl ester (R2). Second row, left to right: tetraethylrhodamine hexyl ester (R6), tetraethylrhodamine octadecyl ester (R18). Third row: sodium dodecyl sulfate (SDS), Fourth row: cetyltrimethylammonium bromide (CTAB), Bottom row: polyethylene glycol 400 dodecyl ether (Thesit[®]).

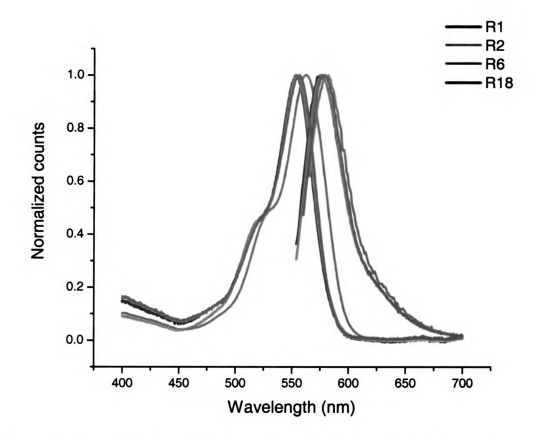


Figure 4.2 - Absorbance and fluorescence spectra of the rhodamine esters used in this study.

If such a sterically mediated interaction does account for our spectral data, it remains unclear why the same spectral shifts are not seen for R18, and this is a matter that bears further investigation. Semi-empirical calculations (HyperChem® v. 6.0) predict no anomalous red-shift for long chain rhodamine esters. Thin layer chromatography (TLC) experiments show no unresolved impurities in our raw material and no other indications of anomalies were apparent in our solution preparation procedures.

Time Resolved Spectroscopy. Experimental time-domain data ($I_{\parallel}(t)$ and $I_{\perp}(t)$) are combined according to Eq. 4.1 to produce the induced orientation anisotropy function, R(t).

$$R(t) = \frac{I_{\parallel}(t) - I_{\perp}(t)}{I_{\parallel}(t) + 2I_{\perp}(t)}$$
(4.1)

The functionality of the R(t) decay provides important information on the dynamics of the chromophores. All of the rhodamine esters exhibit single exponential anisotropy decays in water and biexponential decays in micellar environments. Our previous work has shown that the $S_1 \leftarrow S_0$ transitions we access are oriented along the rhodamine chromophore long axis. In water, the rhodamine esters behave as prolate rotors. For all data, the reported zero-time anisotropies are derived from the regression of the data for times greater than 15 ps after excitation, and the uncertainties reported for each quantity are 95 % confidence intervals for six or more individual determinations. We report the quantities R(0) and τ_{OR} for the rhodamine esters in aqueous and micellar environments in Table 4.1.

The data we present in this paper for the reorientation of the rhodamine esters in water (Figure 4.3) are predicted reasonably well by the well-established Debye-Stokes-

Einstein (DSE) model in the stick limit.³⁴ We note that R18 reorients on a time scale that is faster than the other rhodamine esters and is indeed faster than that predicted by the modified DSE model. We understand this behavior based on the length of the alkyl chain of the ester which interacts with the main portion of the chromophore in such a manner as to screen the ionic charge of the chromophore, thus promoting more "slip" like behavior³⁵ of the chromophore. Thus, even though the hydrodynamic volume^{36,37} of the chromophore increases, the frictional interaction decreases in such a way as to compensate for the change in probe volume.

Table 4.1 – Reorientation times and zero-time anisotropies for Rhodamine chromophores in aqueous and micellar environments.

and inico	llar environm	Water	SDSb	CTAB ^b	Thesit 65
R1	R ₁ (0)	0.25±0.03	0.05±0.02	0.29±0.01	0.32±0.04
	τ ₁ (ps)	132±15	243±118	152±13	160±6
	R ₂ (0)	-	0.27±0.03	0.02±0.01	0.04±0.01
	τ ₂ (ps)	•	1037±48	1405±399	1558±298
	R ₁ (0)	0.22±0.03	0.05±0.02	0.34±0.03	0.30±0.01
R2	$\tau_1(ps)$	129±15	311±111	166±3	151±9
R2	R ₂ (0)	•	0.26±0.02	0.01±0.01	0.04±0.02
	τ ₂ (ps)	•	1024±120	1869±494	1558±207
	R ₁ (0)	0.27±0.04	0.03±0.01	0.23±0.02	0.13±0.04
R6	$\tau_1(ps)$	172±32	97±14	200±31	87±34
KO	R ₂ (0)	•	0.28±0.01	0.08±0.02	0.23±0.02
	τ ₂ (ps)	•	1142±32	1481±543	1361±59
	R ₁ (0)	0.22±0.03	0.02±0.02	0.17±0.02	0.23±0.01
R18	$\tau_1(ps)$	145±21	190±88	149±18	200±21
W10	R ₂ (0)	•	0.25±0.01	0.14±0.01	0.08±0.02
	τ ₂ (ps)	•	1101±36	1275±92	2189±676

a. The data are the best fit results of the data to the function $R(t) = RO(0)\exp(-t/\tau cr)$. Time constants are in ps and the uncertainties are standard deviations $(\pm 1\sigma)$ for at least six determinations of each quantity.

b. The values reported are the best fit results of the data to the function $R(t) = R1(0)\exp(-t/\tau 1) + R2(0)\exp(-t/\tau 2)$. Time constants are in ps and the uncertainties are standard deviations ($\pm 1\sigma$) for at least six determinations of each quantity.

The reorientation data presented here for the rhodamine esters in micellar environments are different for those of the reorientation of these same chromophores in water, with biexponential anisotropy decays being seen for reorientation in micellar solutions (Figures 4.4-4.6). This biexponential behavior is indicative of the intrinsic complexity of these heterogeneous micellar systems. The simplest interpretation of the data suggests that the chromophore reorients either in the water portion of the environment or within the micelles. Examination of the experimental data shows this not to be the case. The reorientation times of the short-time component do not match those for reorientation in water, indicating that the simplest model is not applicable to the treatment of these data. The next layer of complexity accounts for the motion of the chromophore within the micelle as well as the motion of the micelle as a whole. In this model, the chromophore is bound at or near the surface of the micelle, yielding a time constant of τ_w that is related to restricted motion analogous to that of a hindered rotor and τ_m for overall reorientation of the cone equal to micellar motion. The anisotropy function for this model is shown in Eq. 4.2,

$$R(t) = R(0)[S^{2} + (1 - S^{2}) \exp(-t/\tau_{w})] \exp(-t(1/\tau_{d} + 1/\tau_{m}))$$
 (4.2)

where R(0) is the zero-time anisotropy, S is an order parameter, sensitive to the equilibrium orientational distribution width of the chromophore transition moment in its restricted volume and τ_d is considered to be representative of the translational motion of the chromophore about the surface of the micelle. In this model, there are three time constants, but two are amenable to direct determination by virtue of the form of Eq. 4.2. Previous work in the Blanchard group has shown that this expression does in fact model the dynamics of bound and confined chromophores accurately. Sensor Legislation 1.

can be a qualitative correspondence made between the slow time constant arising from motion related to the micelle and the fast time constant related to motion associated with the probe in an environment where it is free to wobble, and we can estimate the partitioning operative in these systems. In this picture, the chromophore aliphatic tail interacts within the inner micelle, and the probe is tethered to the micelle. The length of the tether controls the chromophore proximity to the micelle and thus its freedom of motion. The distribution of the chromophore between a primarily aqueous and a primarily micellar environment can be estimated through the normalized pre-exponential factors $(R_1^*$ and R_2^* for short- and long-time component pre-exponential factors) as shown in Eq. 4.3.

$$R_{1}^{*} = \frac{R_{1}}{R_{1} + R_{2}}$$

$$R_{2}^{*} = \frac{R_{2}}{R_{1} + R_{2}}$$
(4.3)

This treatment assumes that the transition moment angle characteristic of a given chromophore does not depend sensitively on its local environment and, for the systems we consider here, this is likely to be an excellent approximation.⁴⁴

The experimental data for the reorientation of the chromophores in anionic SDS micellar solution (33 mM, 4x cmc) are shown in Figure 4.4, (Table 4.1) and show that R(t)

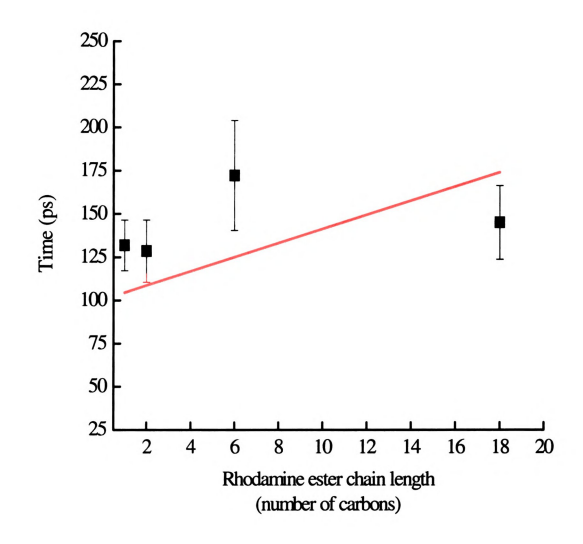


Figure 4.3 - Time-resolved reorientation data for rhodamines in the aqueous phase. Squares (a) are experimental data points and the solid line represents the theoretical reorientation calculated from the Debye-Stokes-Einstein equation.

decays biexponentially to within our ability to determine. For all of the rhodamine esters, we recover the same time constants, to within the experimental uncertainty. The average of the two decays, 210 ± 82 ps and 1076 ± 59 ps, is measurably different than the average reorientation time seen for water (144 \pm 21 ps), despite the fact that the bulk viscosity of the SDS solution is essentially the same as that of water. This finding suggests that there is an interaction of the rhodamines with the micelle, which we would expect based on charge association arguments alone, but which does not allow us to elucidate the nature of the interaction in a direct fashion. The overall motion of SDS micelles is predicted to be on the several nanosecond time scale, ^{14,15,43} and the ~1100 ps time constant we recover appears to be too fast to account for micelle motion. The chromophores do not yield time constants consistent with being bound rigidly in the micelle, or free to rotate in an aqueous environment. Since the slow time constant is not consistent with motion of the free chromophore in bulk water, this leaves the quasi-translational motion of the chromophore along the outer extent of the micelle as the only physical model consistent with the recovered slow time constant. 13,14,16 We can use this model to estimate the energetics of partitioning in these systems.

We assert that fast motion is indicative of the cationic rhodamine chromophore head group existing in a region somewhat separated from the micelle, and that the slow motion is reflective of the rhodamine chromophore that is tightly associated with the micelle. Thus the normalized anisotropy prefactors R_1^* and R_2^* are proportional to the concentrations of the loosely bound (C_1) and tightly bound species (C_t), respectively. If there exists a dynamic equilibrium between these association conditions, we can use the

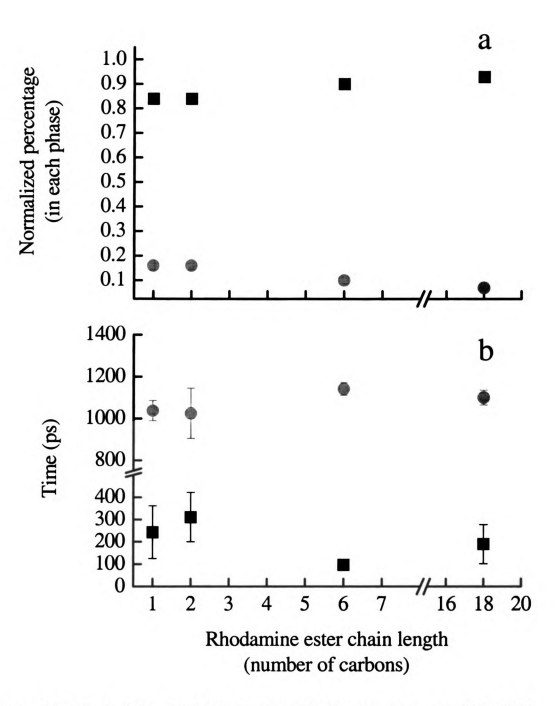


Figure 4.4 – Reorientation data for rhodamine aliphatic esters in aqueous SDS micelle solution. Biexponential anisotropy decay functions produced a) normalized prefactors for the contribution of the fast (\circ) and slow (\bullet) components of the anisotropy decays. b) Reorientation time constants plotted as a function of increasing ester chain length.

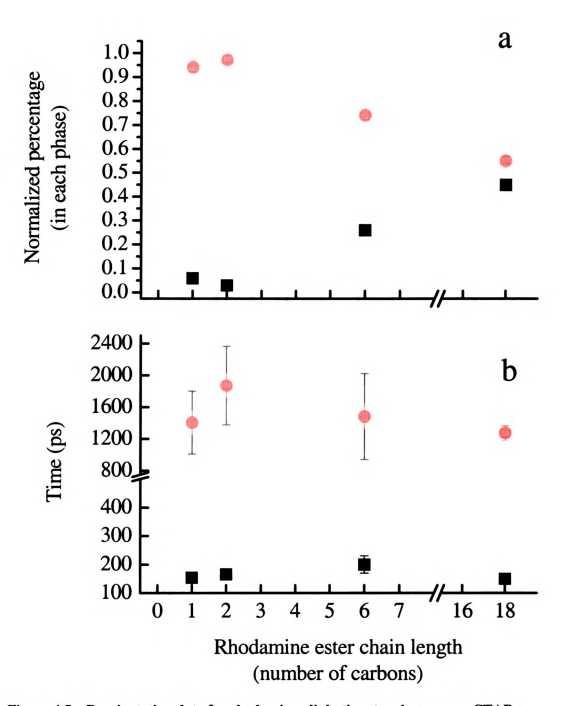


Figure 4.5 – Reorientation data for rhodamine aliphatic esters in aqueous CTAB micelle solution. Biexponential anisotropy decay functions produced a) normalized prefactors for the contribution of the fast (c) and slow (m) components of the anisotropy decays. b) Reorientation time constants plotted as a function of increasing ester chain length.

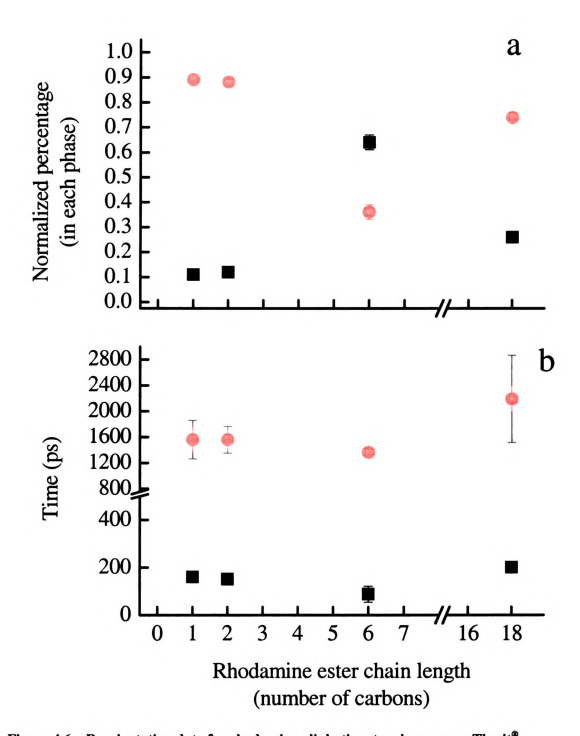


Figure 4.6 – Reorientation data for rhodamine aliphatic esters in aqueous Thesit $^{\bullet}$ micelle solution. Biexponential anisotropy decay functions produced a) normalized prefactors for the contribution of the fast (\circ) and slow (a) components of the anisotropy decays. b) Reorientation time constants plotted as a function of increasing ester chain length.

concentration ratios to obtain the equilibrium constant, which is related to the free energy of interaction between the micelle and chromophore.

$$C_{l} \rightleftharpoons \stackrel{K_{eq}}{=} C_{l}$$

$$K_{eq} = \frac{[C_{l}]}{[C_{l}]} \approx \frac{R_{2}^{*}}{R_{1}^{*}}$$
(4.4)

$$\Delta G = -RT \ln K_{eq}$$

The free energy we extract from these data can be decomposed into ionic and dispersion contributions.

$$\Delta G = \Delta G_{ionic} + \Delta G_{dispersion} \tag{4.5}$$

We can estimate the dispersion contribution as follows. For highly ordered aliphatic chains, such as alkanethiol monolayers, the energy of interaction between chains is taken to be ~ -1.25 kJ/mol-CH₂. 40.41 We believe this value to be too high for micellar systems owing to the substantially lower extent of aliphatic chain ordering in these systems. We estimate the strength of interaction to be -0.5 kJ/mol-CH₂ unit, and calculate the ionic contribution to the interaction energy as a function of rhodamine alkyl ester chain length. We present these calculated results for SDS and CTAB micelles in Table 4.2. The partitioning data reveal that the interaction with the headgroup region is significant, and the dependence of the data on rhodamine alkyl ester chain length reveals the important role of the double layer around the perimeter of the micelle. We will return to a detailed discussion of these results after considering the reorientation data for the esters in each micellar environment.

Table 4.2 – Various thermodynamic properties of Rhodamine chromophores in SDS and CTAB micellar environments.

	SDS					СТАВ				
	Keq	ΔG_{total} $(kJ/mol)^a$	ΔG _{disp} (kJ/mol) ^a	ΔG _{louic} (kJ/mol) ^a	K _{eq}	ΔG _{total} (kJ/mol) ^a	ΔG _{disp} (kJ/mol) ^a	ΔG _{lonic} (kJ/mol) ^a		
R ₁	5.25	-4.14	-0.5	-3.64	0.06	+6.86	-0.5	+7.36		
R ₂	5.25	-4.14	-1.0	-3.14	0.03	+8.67	-1.0	+9.67		
R ₆	9.0	-5.48	-3.0	-2.48	0.35	+2.61	-3.0	+5.61		
R ₁₈	12.5	-6.30	-9.0	+2.70	0.82	+0.5	-9.0	+9.50		

a Values for ΔG_{total} are calculated from Eq. 4.4. Values for ΔG_{ionic} are calculated from Eq. 4.5.

The reorientation dynamics of the rhodamine esters in cationic CTAB micellar solution (3.0 mM, 3x cmc) are shown in Figure 4.5. Again, there seems to be no clear dependence of the reorientation time (Table 4.1) on increasing ester chain length and, although the short time constant that is recovered is closer in absolute value to that for bulk water, it is clear from the biexponential decay dynamics that there is a significant interaction between the CTAB micelles and the chromophores. As with reorientation in SDS micelles, the recovered time constants do not correspond to independent motion of the chromophores within the micelle (too fast), or the motion of the micelle itself (too slow).

When the data on chromophore distribution are examined, a clear picture emerges of increasing chromophore interaction with CTAB as a function of increasing ester chain length (Figure 4.5a). Much like the SDS micelles, the interaction is primarily with the headgroup region for the methyl and ethyl esters, and then increases substantially for the hexyl and octadecyl esters. This effect is dominated by the increase in dispersion interactions between the micelle aliphatic region and the chromophore ester alkyl chains. The effects of ionic interactions are compensated substantially by the presence of the double layer at the micelle perimeter. From the results for ionic interaction energies reported in Table 4.2, it can be seen that the strength of ionic interactions remain

relatively constant and repulsive with increasing probe alkyl chain. Specifically, we recover an ionic interaction energy term for probe-SDS systems that becomes increasingly unfavorable with increasing probe alkyl chain length, and an ionic interaction remains approximately constant for interactions between CTAB and the rhodamine probes. While intuition would suggest strongly attractive ionic interactions between the probe and SDS, with the overall interaction increasing in strength as the probe alkyl ester length increased, this is not what is seen experimentally. We find approximately constant total interaction energy for the probes with SDS, with ionic interactions becoming increasingly unfavorable with increasing alkyl chain length. For these systems, the dominant ionic interactions are between the probe cationic moiety and the double layer at the perimeter of the micelle. For SDS, the counterions are Na⁺ and H⁺ and these ions will interact repulsively with the cationic rhodamine. As the probe alkyl ester chain length is increased, the probe is drawn more efficiently into the micelle and repulsive interactions between the micelle double layer and the probe head group become more pronounced. For CTAB, the opposite result is obtained. The ionic interactions between the rhodamine probe and the CTAB counter ions in the proximity of the micelle head groups remain essentially constant (~8.5 kJ/mol) as a function of rhodamine alkyl ester chain length. For CTAB, the ionic interactions are essentially constant and appear to be mediated by the presence of the counterions at the micelle surface. We note that, despite the importance of ionic interactions being between the micelle counter ions and the cationic probe, the magnitude of the interactions for both systems are similar, and modest.

system (1.0 mM, 10x cmc), it is not clear how the balance of forces will operate, *i.e.* whether polar and dispersion interactions will act in a cooperative or opposing manner. The recovered time constants (Table 4.1) reveal that interaction seems to increase slightly with increasing ester chain length. However, an inspection of the individual time constants for rhodamine reveals that the interaction between the chromophores and the micellar system is anomalous for the hexyl ester. There is a decrease in the time constants measured for R6 and this behavior is unique to the R6/Thesit® system. This trend is also seen in the chromophore partitioning data (Figure 4.5). Starting with the ethyl ester, there is an increase in the chromophore partitioning into the micelle to the point where the chromophore is interacting with the core more strongly than with the headgroup. This trend is reversed for R18, counter to any predictions that can be made based solely on energetic trends.

Wobbling-in-a-Cone with Translational Diffusion and Micelle Rotation. With the partitioning issues understood, we consider next the time constants of the anisotropy decays we measure. We expect that the reorientation time constant for a micelle is several nanoseconds, and we do not observe any such long-time anisotropy decay in our data. The possible reasons for this absence are either a lack of sensitivity to a long-time component, which is not reasonable given the sensitivity and the time resolution of our TCSPC system, or that the persistence time of the interactions between chromophore and micelle is shorter than the reorientation time of the micelle. This explanation is consistent with the modest interactions between the chromophore and the micelle (vide infra). We extract the wobbling diffusion constant D_w using the experimental quantities

 τ_w and S' using Eq. 4.2 and 4.6-4.7. The quantities θ_0 , the confining cone angle and D_w in water $D_w = (6\tau_{cor})^{-1}$ are reported in Table 4.3.

$$D_{w} = \{\tau_{w}(1 - S^{2})\}^{-1}[-\cos^{2}\theta_{0}(1 + \cos\theta_{0})^{2}\{\ln[(1 + \cos\theta_{0})/2] + (1 - \cos\theta_{0})/2\}\{2(1 - \cos\theta_{0})\}^{-1} + (1 - \cos\theta_{0})$$

$$\times (6 + 8\cos\theta_{0} - \cos^{2}\theta_{0} - 12\cos^{3}\theta_{0} - 7\cos^{4}\theta_{0})/24]$$

$$(4.6)$$

$$S' = 0.5\cos\theta_0(1+\cos\theta_0) \tag{4.7}$$

Table 4.3 - Wobbling constant (D_w) values for aqueous and D_w and θ_0 micellar environments.

		R1	R2	R6	R18
Water	$D_w (x10^9 Hz)$	1.26	1.30	0.97	1.15
SDS	$D_w (x10^9 Hz)$	0.66	0.46	2.15	1.03
SUS	θ_0	58.7	58.2	64.3	67.0
CTAD	$D_w (x10^9 \text{ Hz})$	0.07	0.03	0.23	0.58
CTAB	θ_0	12.0	8.0	25.2	35.3
Thesit®	$D_w (x10^9 \text{ Hz})$	0.12	0.14	1.57	0.24
i nesit	θ_0	16.0	16.5	45.2	25.2

The values of the order parameter, S' vary from 0.84 to 0.94 for reorientation of the rhodamine esters in the micelles. The order parameter is a measure of the time-averaged orientational distribution of the chromophores and can take on values from zero for a completely random distribution of chromophores to one for a rigid crystalline system. Our derived values for S' indicate that, on average, the micellar systems are well ordered with the order increasing from the neutral to cationic, to anionic micelles. These data are related to the values recovered for the cone angles associated with the wobbling chromophores. For SDS micelles, the cone angle decreases with increasing ester chain length, indicating more confinement of the chromophore, consistent with our calculations of the ionic interaction energy. For CTAB micelles, the cone angle becomes larger with increasing chromophore aliphatic chain length, again in keeping with the energetic

estimates. We view the interaction of the chromophore in the micelle as an activated process, so its residence time and thus the measured cone angle will scale with the overall energy of interaction. For the Thesit[®] micelles, substantial disorder exists, as is seen by the larger cone angles present for the very short chain esters and the rapid increase in diffusion coefficient with increasing probe alkyl chain length. While the diffusion coefficients for the chromophores in water decrease with ester size, this is an expected result and is due to increasing correlation times in the bulk water. The esters are free to reorient about their tethering bonds as indicated by the quantities of wobbling diffusion coefficient, D_w, which also indicate that there is substantial confinement in these systems. The value of D_w in micelles is 6-9 times slower than that for the free chromophores in water, but it is important to keep in mind that the free volume accessible to the chromophores in the micelle is substantially less than that of the same chromophores in water.

Conclusion

We have studied the steady state spectroscopy and reorientation dynamics of selected rhodamine esters in water and in the aqueous micellar systems, SDS, CTAB and Thesit[®]. The charges of the rhodamines and the lengths of the ester chains dictate that there is an interaction with each of these micellar systems and we have used this interaction to probe the balance of forces operating between micelles and amphiphilic probes. The reorientation dynamics of the chromophores are consistent with translational motion of the tightly bound chromophore along the surface of the micelle and less restricted motion of the chromophore when it is tethered less tightly to the micelle. Our data indicate that there is indeed a balance of forces between the ionic moieties in the

headgroup region and the dispersion forces that characterize the inner core region. For the ionic micelles, the role of the double layer formed by counter-ions is substantial in mediating repulsive or attractive ionic interactions. For Thesit[®], the absence of an ionic double layer and the presence of substantial disorder in the mantle region gives rise to behavior that is qualitatively consistent with that seen in the ionic micelles, but differing in detail. It is clear from these data that, for ionic micelles, the presence of counter ions to form a double layer near the micelle head groups serves to mediate ionic interactions. Because of this ionic compensation effect, the role of dispersion interactions assume substantial importance in determining the dynamics of micellar media. An important issue will be to consider the extent to which this balance of forces is altered in a two-dimensional amphiphilic system.

Acknowledgment

We are grateful to the National Science Foundation for their support of this work through Grant 0090864.

Literature Cited

- (1) Jarzeba, W.; Walker, G. C.; Johnson, A. E.; Kahlow, M. A.; Barbara, P. F. J. Phys. Chem. 1988, 92, 7039.
- (2) Visser, A. J. W. G.; Vos, K.; van Hoek, A.; Santema, J. S. J. Phys. Chem. 1988, 92, 759.
- (3) Marcus, A. H.; Dichun, N. A.; Fayer, M. D. J. Phys. Chem. 1992, 96, 8930.
- (4) Quitevis, E. L.; Marcus, A. H.; Fayer, M. D. J. Phys. Chem. 1993, 97, 5762.
- (5) Cho, C. H.; Chung, M.; Lee, J.; Nguyen, T.; Singh, S.; Vedamuthu, M.; Yao, S.; Zhu, J.-B.; Robinson, G. W. J. Phys. Chem. 1995, 99, 7806.
- (6) Streletzky, K.; Phillies, G. D. J. Langmuir 1995, 11, 42.
- (7) Nandi, N.; Bagchi, B. J. Phys. Chem. 1996, 100, 13914.
- (8) Maiti, N. C.; Krishna, M. M. G.; Britto, P. J.; Periasamy, N. J. Phys. Chem. B 1997, 101, 11051.
- (9) Matzinger, S.; Hussey, D. H.; Fayer, M. D. J. Phys. Chem. B 1998, 102, 7216.
- (10) Riter, R. E.; Willard, D. M.; Levinger, N. E. J. Phys. Chem. B 1998, 102, 2705.
- (11) Willard, D. M.; Riter, R. E.; Levinger, N. E. J. Am. Chem. Soc. 1998, 120, 4151.
- (12) Pal, S. K.; Mandal, D.; Sukul, D.; Bhattacharyya, K. Chem. Phys. Lett. 1999, 312, 178.
- (13) Bhattacharyya, K.; Bagchi, B. J. Phys. Chem. A 2000, 104, 10603.
- (14) Pal, S. K.; Sukul, D.; Mandal, D.; Sen, S.; Bhattacharyya, K. Chem. Phys. Lett. **2000**, 327, 91.
- (15) Cang, H.; Brace, D. D.; Fayer, M. D. J. Phys. Chem. B 2001, 105, 10007.
- (16) Hara, K.; Kuwabara, H.; Kajimoto, O. J. Phys. Chem. A 2001, 105, 7174.
- (17) Sen, S.; Sukul, D.; Dutta, P.; Bhattacharyya, K. J. Phys. Chem. A 2001, 105, 7495.
- (18) Mandal, D.; Sen, S.; Bhattacharyya, K.; Tahara, T. Chem. Phys. Lett. 2002, 359, 77.
- (19) Dutt, G. B. J. Phys. Chem. B. 2002, 106, 7398
- (20) Berr, S. S.; Caponetti, E.; Johnson, J. S.; Jones, R. R. M.; Magid, L. J. J. Phys. Chem. 1986, 90, 5766.

- (21) Berr, S. S.; Coleman, M. J.; Jones, R. R. M.; Johnson, J. S. J. J. Phys. Chem. 1986, 90, 6492.
- (22) Berr, S. S. J. Phys. Chem. 1987, 91, 4760.
- (23) Kawato, S.; Kinosita Jr., K.; Ikegami, A. *Biochemistry* 1978, 17, 5026.
- (24) Dewitt, L.; Blanchard, G. J.; Legoff, E.; Benz, M. E.; Liao, J. H.; Kanatzidis, M. G. J. Am. Chem. Soc. 1993, 115, 12158.
- (25) Blanchard, G. J.; Wirth, M. J. Anal. Chem. 1986, 58, 532.
- (26) Andor, L.; Lorincz, A.; Siemion, J.; Smith, D. D.; Rice, S. A. Rev. Sci Instrum. 1984, 55, 64.
- (27) Bado, P.; Wilson, S. B.; Wilson, K. R. Rev. Sci Instrum. 1982, 53, 706.
- (28) Ferguson, J.; Mau, A. W. H. Chem Phys. Lett. 1972, 17, 543.
- (29) Rosenthal, I.; Peretz, P.; Muszkat, K. A. J. Phys. Chem. 1979, 83, 350.
- (30) Pevenage, D.; Van der Auweraer, M.; De Schryver, F. C. Langmuir 1999, 15, 8465.
- (31) Kohn, F.; Hofkens, J.; De Schryver, F. C. Chem Phys. Lett. 2000, 321, 372.
- (32) Ghanadzadeh, A.; Zanjanchi, M. A. Spectrochim. Acta, Part A 2001, 57, 1865.
- (33) Drexhage, K. H. In *Dye Lasers*; 2nd ed.; Schaefer, F. P., Ed.; Springer: Berlin, 1977; pp 144.
- (34) Debye, P. Polar Molecules Chemical Catalog Co.: New York 1929.
- (35) Hu, C.; Zwanzig, R. J. Chem. Phys. 1974, 60, 4354.
- (36) Youngren, G. K.; Acrivos, A. J. Chem. Phys. 1975, 63, 3846.
- (37) Fleming, G. R.; Knight, A. E. W.; Morris, J. M.; Robbins, R. J.; Robinson, G. W. Chem. Phys. Lett. 1977, 51, 399.
- (38) Horne, J. C.; Blanchard, G. J. J. Am. Chem. Soc. 1996, 118, 12788.
- (39) Horne, J. C.; Blanchard, G. J. J. Am. Chem. Soc. 1998, 120, 6336.
- (40) Horne, J. C.; Blanchard, G. J. J. Am. Chem. Soc. 1999, 121, 4427.
- (41) Horne, J. C.; Blanchard, G. J.; Legoff, E. J. Am. Chem. Soc. 1995, 117, 9551.
- (42) Horne, J. C.; Huang, Y.; Liu, G. Y.; Blanchard, G. J. J. Am. Chem. Soc. 1999, 121, 4419.

- (43) Kelepouris, L.; Blanchard, G. J. J. Phys. Chem. B 2002, 106, 6600.
- (44) Kelepouris, L.; Krysinski, P.; Blanchard, G. J. J. Phys. Chem. B. 2002, In submission.

Chapter 5

Conclusions and Future Work

In this dissertation we have studied the reorientation dynamics of Rhodamine chromophores in polar protic and aprotic, associative condensed phases and in micellar systems. We have examined the dynamics of these chromophores in *n*-alcohols, methanol to decanol, the polar aprotic solvents acetonitrile, DMF and DMSO, aqueous environments and finally the cationic, anionic and neutral micellar environments of SDS, CTAB and Thesit[®]. These studies have been conducted to better understand local organization in restricted, condensed phases and to gain a better understanding of the interactions that occur in polar, strongly associative systems.

We now better understand the role of local heating, which changes the viscosity of the liquid. We have studied this effect (Chapter 2) in polar protic environments and understand how this effect can be attributed to the excess excitation energy given to the molecule in terms of a local heating affect. A better understanding of this phenomenon could be achieved by extending this work to other environments and other chromophores. Future work would include investigating the reorientation dynamics of different chromophores and different solvents to understand if the local heating effect is localized to the rhodamine chromophores that we studied, or is a more generalized effect that is observable in a broad range of environments.

Chapter 3 detailed experiments involving the use of solute structure and solvent functionality to probe intermolecular interactions that occur on molecular length scales.

We understand these interactions in the context of the environments that we have studied, but recognize that this work can be extended to include other environments in order to

better probe the interactions that we have studied. Specifically, extensions of this work are required to include a broader range of aprotic environments, environments that sample specific regions of the viscosity range and different structural environments in order to probe the structure-solvation relationship. We understand the hydrogen bonding interactions that occur between the nitrogen, oxygen and hydrogen atoms in condensed phases in the context of these measurements, but a need to extend this work to other types of functional groups exists. Only through extending these measurements to other functional groups can we complete a picture of structure and local organization in condensed phases.

Chapter 4 of this dissertation detailed work involving the interactions of Rhodamine esters and micellar systems. We examined the interaction of four different esters in cationic, anionic and neutral systems in order to gain a better understanding of the balance of forces that are present in these systems. We understand the interactions of the cationic Rhodamine esters with the anionic SDS micelles and to an extent with the cationic CTAB micelles, where the longer ester chains balance the repulsive forces that are present between the chromophores and the headgroups of the micelle. We have a limited understanding of the interactions that occur in the neutral micellar system,

Thesit®, because of the nature of the interactions that we have observed. We understand that this system is the most disordered of the three systems that we have chosen to study and believe that this disorder contributes to the observed interactions such that the chromophores have greater degrees of freedom than in either the cationic or anionic systems. Several different length scales of ester (propyl, butyl, heptyl or octyl esters, for instance) could be employed to probe this effect further and to better understand the

interactions that occur not only in the neutral system, but also the cationic and anionic systems.

The information gathered in the pursuit of this dissertation has provided a contribution toward the understanding of local organization in condensed phases and allowed the notions of local heating, hydrogen bonding, dielectric friction and solute-solvent interactions to be probed in the context of the reorientation dynamics of Rhodamine chromophores.

